

University of Alberta

Catalytic and kinetic study of
methanol dehydration to dimethyl ether

by

Seyed Shaham Aldin Hosseininejad

A thesis submitted to the Faculty of Graduate Studies and Research
in partial fulfillment of the requirements for the degree of

Master of Science
in
Chemical Engineering

Chemical and Materials Engineering

©Seyed Shaham Aldin Hosseininejad

Fall 2010
Edmonton, Alberta

Permission is hereby granted to the University of Alberta Libraries to reproduce single copies of this thesis and to lend or sell such copies for private, scholarly or scientific research purposes only. Where the thesis is converted to, or otherwise made available in digital form, the University of Alberta will advise potential users of the thesis of these terms.

The author reserves all other publication and other rights in association with the copyright in the thesis and, except as herein before provided, neither the thesis nor any substantial portion thereof may be printed or otherwise reproduced in any material form whatsoever without the author's prior written permission.

Examining committee

Robert E. Hayes, Chemical and Materials Engineering

Artin Afacan, Chemical and Materials Engineering

Natalia Semagina, Chemical and Materials Engineering

Jason Olfert, Mechanical Engineering

Research is what I'm doing when I don't know what I'm doing

- Werner von Braun

DEDICATION

I would like to dedicate this work to my parents and my friends. To my parents who inspired me to come this far.

ABSTRACT

Dimethyl ether (DME), as a solution to environmental pollution and diminishing energy supplies, can be synthesized more efficiently, compared to conventional methods, using a catalytic distillation column for methanol dehydration to DME over an active and selective catalyst.

In current work, using an autoclave batch reactor, a variety of commercial catalysts are investigated to find a proper catalyst for this reaction at 110-135 °C and 900 kPa. Among the γ -Alumina, Zeolites (HY, HZSM-5 and HM) and ion exchange resins (Amberlyst 15, Amberlyst 35, Amberlyst 36 and Amberlyst 70), Amberlyst 35 and 36 demonstrate good activity for the studied reaction at the desired temperature and pressure. Then, the kinetics of the reaction over Amberlyst 35 is determined. The experimental data are described well by Langmuir-Hinshelwood kinetic expression, for which the surface reaction is the rate determining step. The calculated apparent activation energy for this study is 98 kJ/mol.

ACKNOWLEDGEMENT

First, I would like to express the deepest appreciation to my supervisor, Dr. Robert E. Hayes, who has supported me throughout my thesis with his patience and knowledge. Working with Dr. Hayes has been not only an honor for me but also one of the most significant opportunities that I have ever had in my whole life.

I gratefully acknowledge Artin Afacan for his advice, supervision, and crucial contribution, which made him a backbone of this research and so to this thesis. I am grateful in every possible way and hope to keep up our collaboration in the future.

I would like to thank Dr. Karl T. Chuang for his technical support during my experiments. I have also benefited by advice and guidance from Christina, Rajab and Fariborz who always kindly grant me their time.

I also want to acknowledge Biorefining conversions network for financial support and for giving me the opportunity to work on this project.

Finally, I would like to thank my family whose help and encouragement in the most terrible moments has been always my greatest property.

TABLE OF CONTENTS

Chapter 1 <i>Introduction</i>	1
Chapter 2 <i>Background and Literature Review</i>	4
2.1. DME Properties	5
2.1.1. Physical and thermo-physical properties	5
2.1.2. Health, safety and environmental issues	6
2.2. DME applications	7
2.2.1. DME as Fuel	8
2.2.2. DME as Energy carrier	9
2.2.3. DME as intermediate	10
2.3. DME synthesis	10
2.3.1. DME from synthesis gas	11
2.3.2. Production processes	12
2.4. Catalytic methanol dehydration	14
2.4.1. Solid-acid catalysts	14
2.4.2. Reaction kinetics	19
2.5. Summary	21
Chapter 3 <i>Material and Methods</i>	23
3.1. Catalysts and other Chemicals	23
3.2. Vacuum Dryer	25
3.3. Reactor	26
3.4. Sample analysis	28

3.5. Acidity Determination	31
3.6. Experimental Procedure.....	32
3.6.1. Calculations.....	32
3.6.2. Error Analysis	35
Chapter 4 <i>Results and Discussion</i>	38
4.1. Kinetic Studies for Amberlyst 35	46
4.1.1. Reproducibility	47
4.1.2. The effect of initial reactant mass to catalyst mass ratio	48
4.1.3. The effect of external and internal diffusion.....	50
4.1.4. The effect of methanol concentration on reaction rate	51
4.1.5. The effect of initial water concentration on reaction rate	52
4.2. Kinetics Modeling.....	53
Chapter 5 <i>Conclusion and Recommendations</i>.....	62
References	64
Appendix A <i>Experimental data</i>	70
Appendix B <i>Sample calculation and error analysis</i>	72
Appendix C <i>Acidity measurements for Amberlysts</i>	76
Appendix D <i>Mechanism study for Amberlyst 35</i>	80

LIST OF TABLES

Table 2.1 Properties of DME in comparison with some other fuels.....	6
Table 2.2 Life time and global warming potentials of DME and other compounds	7
Table 2.3 Properties of DME and LPG.....	9
Table 2.4 Kinetic models studied for methanol dehydration to DME.....	19
Table 3.1 Properties of three different Zeolites catalysts	24
Table 3.2 Amberlyst series catalysts properties.....	25
Table 3.3 Area percent of methanol and known weight percent of methanol	29
Table 3.4 The GC calibration for three tetrahydrofuran concentrations.....	30
Table 4.1 Comparison of DME produced as a function of time for four runs.....	47
Table 4.2 The initial reaction rate per gram of catalyst and final methanol % conversions for three different reactant mass to catalyst mass ratios.	50

LIST OF FIGURES

Figure 2.1 Different sources for DME synthesis	11
Figure 2.2 Bimolecular mechanism of methanol dehydration on an acid-base pair (Spivey,1991).....	15
Figure 2.3 Gates and Johanson (1969) mechanism for methanol dehydration reaction.....	20
Figure 2.4 Kiviranta-Paakkonen (1998) mechanism for methanol dehydration reaction.....	21
Figure 3.1 The vacuum dryer used to remove water from the catalyst samples..	26
Figure 3.2 Schematic of the batch reactor used in this study.....	27
Figure 3.3 GC calibration curve for methanol-water solutions	29
Figure 3.4 GC calibration curves for methanol-water-THF solutions.....	31
Figure 4.1 DME moles produced over Amberlyst 70 and H-ZSM-5 at 150 °C and 1.7 MPa.....	39
Figure 4.2 Methanol conversion over Amberlyst 70 and H-ZSM-5 at 150 °C and 1.7 MPa.....	40
Figure 4.3 DME moles produced over Amberlyst 15, Amberlyst 35, Amberlyst 36 and Amberlyst 70 at 110 °C and 900 kPa using pure methanol as feed	41
Figure 4.4 Methanol conversion over Amberlyst 15 Amberlyst 35 (Amberlyst 36 and Amberlyst 70 at 110 °C and 900 kPa using pure methanol as feed	41
Figure 4.5 DME moles produced over Amberlyst 15 Amberlyst 35 Amberlyst 36 and Amberlyst 70 at 130 °C and 900 kPa using pure methanol as feed	42
Figure 4.6 Methanol conversion over Amberlyst 15 Amberlyst 35 Amberlyst 36 and Amberlyst 70 at 130 °C and 900 kPa using pure methanol as feed	43

Figure 4.7 2.5M water in methanol solution as feed to reactor for methanol dehydration reaction over Amberlysts at 130 °C and 900kPa.....	44
Figure 4.8 3.5M water in methanol solution as feed to reactor for methanol dehydration reaction over Amberlysts at 130 °C and 900kPa.....	44
Figure 4.9 Initial reaction rate for pure methanol, 2.5M and 3.5M water solutions over Amberlyst 15, 35, 36 and 70 at 130 °C and 900kPa.....	45
Figure 4.10 The initial reaction rate of DME production as a function of catalyst acidity for Amberlyst 15, 35, 36 and 70 at 110 °C using pure methanol as feed .	46
Figure 4.11 Moles of DME produced at 130 °C and 900 kPa using pure methanol as feed for four runs	48
Figure 4.12 DME synthesized for different initial reactant mass/catalyst mass ratios of 120/4, 120/6, and 180/8 at 130 °C and 900 kPa using pure methanol as feed.....	49
Figure 4.13 The DME produced moles over different Amberlyst catalyst particle sizes at 130 °C and 900 kPa using pure methanol as feed including the water from the catalyst	51
Figure 4.14 Effect of methanol concentration on initial reaction rate at different temperatures and 900 kPa for different concentrations of methanol/THF solutions	52
Figure 4.15 Effect of water concentration on initial reaction rate at 130 °C and 900 kPa using different concentrations of methanol/water solutions as feed	53
Figure 4.16 Left hand side of Equation (4.8) versus methanol concentration.....	55
Figure 4.17 Left hand side of Equation (4.7) versus methanol concentration.....	56
Figure 4.18 Arrhenius plot for methanol dehydration reaction at temperature range of 110 - 135 °C and 900 kPa using pure methanol as feed	57

Figure 4.19 Left hand side of Equation (4.14) versus $(C_W^{0.5}/C_M)$	59
Figure 4.20 Left hand side of Equation (4.14) versus (C_W/C_M)	59
Figure 4.21 $\ln(K_W / K_M)$ versus $1/T$ in temperature range 110-135 °C and 900 kPa using 3.5 M water/methanol solution as feed	61

ACRONYMS

CD	Catalytic Distillation
CFC	Chlorofluorocarbon
CI	Compression Ignition
DDMEFC	Direct DME Fuel cell
DEE	Diethyl Ether
DME	Dimethyl Ether
DMFC	Direct Methanol Fuel Cell
ER	Eley-Rideal
GC	Gas Chromatography
GHG	Green House Gas
ICE	Internal Combustion Engine
ICI	Imperial Chemical Industries
LH	Langmuir-Hinshelwood
LPG	Liquefied Petroleum Gas
PM	Particulate Matter
PTFE	Poly Tetrafluoroethylen
SI	Spark Ignition
STD	Syngas to DME
Syngas	Synthesis Gas
TCD	Thermal Conductivity Detector
VOC	Volatile Organic Compound
WTW	Well to Wheel

Chapter 1

Introduction

Global warming and the diminishing of traditional energy sources are likely two major concerns of scientists, engineers and governments. In the area of transportation fuels, the way of diesel-based systems and modified diesel fuels (e.g. reduced sulphur content and adding oxygenate) with better combustion properties are being studied by scientists and engineers. In addition to an increased switch from gasoline to diesel, the use of alternative fuels is also being considered. A proper alternative fuel can reduce the Greenhouse Gases (GHG), Particulate Matter (PM) and NO_x emissions.

In recent decades, many companies, particularly in China and Sweden (e.g. Volvo) have been developing DiMethyl Ether (DME) engines and are researching the use of DME as a substitute fuel for diesel engines. DME has a high cetane number and ignition temperature close to conventional diesel fuels, and can be used in diesel engines with some modification in engine sealing. The manufactured DME engines have shown lower NO_x emission, lower smoke and lower engine noise compared to diesel engines. Moreover, DME is among the high Well-to-Wheel efficiency (WTW) fuels. In addition to alternative fuel, DME can also be used as feed stock to many chemicals and a replacement for Liquefied Petroleum Gas (LPG) because of similar properties.

Recent interests in DME, has inspired many countries in the construction of DME plants. DME international Corp. and DME Development Company have been created to facilitate the introduction of DME as an alternative fuel with a production of 850-1650 kilotons per year. Countries with natural gas resources such as middle-east countries that are far from the consuming centers are interested in DME production as a way of transporting energy to the costumers. Although methane can be used as a source of synthesis gas, which is subsequently transformed to methane and DME, there are many alternative sources for syngas, such as biomass (Olah, 2009).

Traditionally, DME has been produced from synthesis gas (syngas) in a two step process, in which methanol is produced from syngas and purified and then it is converted to DME in another reactor. Topsøe (1985) suggested catalyzing both methanol synthesis and methanol dehydration reactions in a single reactor over a bi-functional catalyst. Many studies have investigated different types of solid-acid catalysts such as γ -alumina and zeolites for this method.

In the conventional method, in order to purify DME synthesized in a fixed-bed reactor, at least two distillation columns are needed. To reduce both capital and operating costs, and to increase energy efficiency, process integration can be considered. Catalytic distillation (CD) is one such integrated process, where the reactor and distillation column are combined into a single unit. CD has been attracting significant attention globally in recent years.

Methanol dehydration to DME (Equation (1.1)) is a reaction compatible to CD. The advantages of using CD for methanol dehydration include a higher selectivity of products to DME synthesis, higher conversion compared to a single reactor and lower operational cost. However, the CD requires operation at moderate temperature and pressure (40-180 °C and 8-12 bar). Most of the catalysts previously studied for this reaction are solid-acid catalysts (e.g. zeolites) active at high temperature (250 °C), and little research has been conducted at the milder conditions required for CD.



The purpose of the present study was to find a suitable commercial catalyst for methanol dehydration to DME reaction at moderate temperature (110-135 °C) and pressure (9 bar). The activity of commercial solid-acid catalyst such as γ -Alumina, HY, HZSM-5, HM zeolites and ion exchange resins (Amberlyst 15, Amberlyst 35, Amberlyst 36, Amberlyst 70) for methanol dehydration to DME using an Autoclave batch reactor is investigated. Then, kinetics of dehydration of methanol to DME over the selected commercial catalyst will be tested in order to determine a reaction kinetic model.

The remainder of the thesis is organized as follows

Chapter 2 presents the background on DME and its relevance in the context of alternative fuels and use as a platform chemical. The relevant literature is reviewed.

Chapter 3 gives a description of the experimental methodology used to determine catalyst activity and develop kinetic rate expressions.

Chapter 4 presents the results; first, the activity comparison for a series of catalysts are given, followed by a detailed kinetic investigation of a single catalyst. The results are discussed in some detail.

Chapter 5 gives the overall conclusions and recommendations.

Chapter 2

Background and Literature Review

Environmental pollution and its prevention have been major concerns of human beings for the past few decades. One of the main sources of air pollution is the exhaust of the car engines. Industrial countries have implemented new regulations aimed to achieve lowering of the gas emission level of automobile engines. One potential approach to this goal is to modify engines and/or fuel injection systems. This approach may be expensive to implement. Another approach is to use an alternative fuel with a lower carbon footprint.

Alcohol-based fuels have been considered important energy sources since the 19th century. As early as 1894, France and Germany were pioneers in using ethanol in Internal Combustion Engines (ICE). Henry Ford, Alexander Graham Bell and Thomas Edison supported the idea. Following the 1973 oil crisis, interest in ethanol in United States surged (Minteer, 2006). Pure methanol, another potential alcohol fuel, has certain environmental advantages compared to conventional diesel fuels although it has lower energy density and cetane number compared to diesel fuels. With pure methanol, engine starting problems occur in cold weather because of its low vapor pressure (Olah et al., 2009). In the 1980s, a solution to this problem was found to use dimethyl ether (DME), which has excellent cold start properties, as an additive to methanol (Kozole and Wallace, 1988).

In the 1990s, DME was used as an ignition aid in Compression Ignition (CI) engines. Methanol, a proper substitute of gasoline in Spark Ignition (SI) engines, is not a good substitute for diesel engines. However, Haldor Topsøe introduced DME suitable for diesel engines with a cetane number 55-60, compared to 45-55 for regular diesel fuel. Currently, DME is mainly used as aerosol propellant and has the potential to be used as alternative fuel for diesel engines, a replacement of LPG, in power generation and fuel cells.

The global demand is increasing rapidly; from 150 kilotons per year in 2004 to 2 million tons per year in 2008 in China alone, which provides a strong incentive for a more efficient DME production process.

In this chapter, DME properties and applications as a background to DME are discussed. This is followed by a literature review on production processes for DME.

2.1. DME Properties

2.1.1. Physical and thermo-physical properties

Dimethyl Ether, the simplest ether, is an organic compound with a chemical formula CH_3OCH_3 . It is a colorless gas at standard temperature with a very mild odor. Thus, it does not require an odorant in its applications, which is, at present, mainly used as a propellant in various spray cans instead of Chlorofluorocarbons (CFC) gases. DME has a boiling point of $-24.9\text{ }^\circ\text{C}$ at 1 atm. However, it is transported and stored in liquid form at higher pressures. The physical properties of DME are similar to LPG such as propane and butane. However, DME has low viscosity which causes many leakage problems during production and storage. Some of the properties of DME are given in Table 2.1.

Table 2.1 Properties of DME in comparison with some other fuels

Property	Dimethyl ether (DME)	Diethyl ether (DEE)	Methanol	Methane	Diesel
Chemical formula	CH ₃ OCH ₃	C ₂ H ₅ OC ₂ H ₅	CH ₃ OH	CH ₄	-
Molecular weight (g/mol)	46.07	74.12	32.04	16.04	190-220
Oxygen content (mass %)	34.8	21.6	50	0	0
Density (kg/m ³) @ 15 °C	668	713	794	0.68	841
Viscosity (kg/m.s) @ 25 °C	0.12-0.15	0.224	0.768		5.35-6.28
Vapor pressure (bar) @ 25 °C	5.3	1.25	0.31	NA	<0.1
Critical pressure (atm)	52	36.7	81	45.96	29.7
Critical temperature (°C)	127	194	239	-83	435
Solubility in water (g/L) @ 20 °C	71	69	miscible	0.035	immiscible
Boiling point (°C) @ 1 atm	-24.9	34.5	64.8	-161.5	180-350
Lower Heating Value (MJ/kg)	28.8		20.1		42.8
Cetane number	55-60	85-96	3	3	45-55
Autoignition temperature (°C)	235	170	460	538	210
Flammability limits in air (vol%)	3.4-27	1.9-36	5.5-36	5-15	0.6-6.5
Flash point (°C)	-41	-45	12	-188	62

2.1.2. Health, safety and environmental issues

DME is non-toxic, non-carcinogenic, non-teratogenic, and non-mutagenic. The main DME exposure to human body occurs by inhalation. According to studies to date, DME seems to have very low reactivity in biological systems. It has no irreversible negative health effect on the human body in neither the short nor the long term (Dupont, 1987).

DME, similar to natural gas, burns with a visible blue flame over a wide range of air/fuel ratios. The flammability limits of DME are 3.4-17 % in air. Peroxides, which are very explosive, are produced when ether is exposed to air. In normal conditions, peroxide formation from DME is very small amount compared to other ethers; however, free radical inhibitor is used to prevent any peroxide formation.

Diesel vehicles are a large source of air pollution generated in transportation especially in Europe. DME is clean burning, producing no soot, black smoke or SO₂, and very low emission of NO_x. DME has no carbon to carbon bond; thus,

there is no particulate matter emission from DME except small amount of particulate matter emission which is made by the lubricating oil used in engine. Environmentally, DME is very friendly compared to other volatile organic compounds (VOC). DME is soluble in water and can contaminate underground sources of water; however, degradation by microorganisms and a low boiling temperature makes water contamination a relatively low concern (Olah et al., 2009). In the air, DME degrades by reacting to hydroxyl and nitrate radicals. The life time of 5.1 days was calculated from the models of fast degradation of DME in atmosphere by hydroxyl radical groups (Olah et al., 2009; Good et al., 1998). Table 2.2 also shows the global warming potential of DME compared to other compounds.

Table 2.2 Life time and global warming potentials of DME and other compounds

Gas	Life time (years)	Time horizon (years)		
		20	100	500
DME ¹	0.015	1.2	0.3	0.1
CO ₂ ²	NA	1	1	1
Methane ²	12	72	25	7.6
N ₂ O ²	114	289	298	153
CFC11(CCl ₃ F) ²	45	6730	4750	1620

¹. From reference Good et al. 1998

². From reference Forster et al. 2007

2.2. DME applications

Today, the environmentally friendly DME is mainly used as the propellant for various spray cans instead of CFC. However, new considerations toward DME as an alternative diesel fuel have attracted industries. DME has properties similar to LPG; therefore, it can be used in LPG applications. DME can also be used in Fuel Cells, in marine fuels, and for static power and heat generation purposes.

2.2.1. DME as Fuel

Methanol and DME both have combustion properties that make them appropriate fuel for SI and CI engines respectively. Methanol, with an octane rating of 100, allows the engine to run at a higher compression ratio and thus giving a higher efficiency compared to gasoline engines. However, methanol has some drawbacks such as half energy density, metal corrosion, and cold start problems, which offset its value for the reduction of NO_x, SO_x and particulate matter emissions. Recent studies have solved a lot of those problems to make the engines compatible with methanol. For example, addition of a volatile component such as DME (boiling point -25 °C) can solve the cold start problem. Later in 1988, Kozole and Wallace found that pure DME, already used as an additive to methanol, is a good fuel for CI engines. Similar to cetane number for diesel fuel (45-55), DME has a cetane number of 55-60. Moreover, DME as an alternative diesel fuel reduces the NO_x and particulate matter emission and lowers the noise of the engine. (Paas, 1997; Arcoumanis et al., 2008)

In the early 1970s, CI engines, with higher compression ratio and better fuel economy, have been used even for personal automobiles. DME vehicles are being developed and tested around the world such as Japan and Sweden. In Sweden, Volvo is working on its third generation DME technology and has manufactured some trucks and buses running with DME. Black liquor, the residuals of pulp production, is a raw material used in DME production. This matter inspires Sweden, a pulp producer, to use DME as diesel fuel in addition to the environmental benefits of DME. In Japan, Isuzu has tested DME-powered buses and trucks which have led to the same conclusions reached by Volvo. They believe that DME technology is going to provide a significant substitute for the diesel fuel. In Shanghai Jiao Tong University of China, researchers estimate the cost of adapting a diesel engine to run on DME at less than \$1200 (Olah et al., 2009)

Although DME offers many significant advantages as an alternative fuel for diesel engines, it also has drawbacks. First, because DME has a lower energy

density than diesel fuel, it needs about double the volume of storage tank to contain the same amount of energy. Second, DME has a low viscosity which can lead to leakage in storage and delivery systems. DME viscosity (0.15 centipoise) lies between the propane (0.10) and butane (0.18) (Paas, 1997). Running engines with LPG have given enough experience to solve this problem using a blend of DME and other components. The other problem with DME is its low lubricity, which might lead to failure of the system. Some additives such as Lubrizol and Hitec 560 are used to increase the lubricity of DME. As with methanol, DME is incompatible with some plastics and rubbers. Therefore, appropriate materials should be chosen to prevent leakage of the system after a long time of exposure to DME. Although the most effective and temperature resisting sealing is non-sparking metal to metal seals; polytetrafluoroethylen (PTFE) and butyl-n rubber are compatible materials used for the sealing of DME systems as well.

2.2.2. DME as Energy carrier

DME and LPG (Liquefied Petroleum Gas): LPG (i.e. propane and butane) is mostly used as a residential fuel for heating and cooking. With growing demand for LPG and a shortage of supplies, some countries are studying DME as a substitute for LPG. Because of similar properties between DME and LPG (Table 2.3), LPG infrastructures can be adapted to DME use with small modifications. With less than 20 % DME blend with LPG, existing LPG infrastructures can be used without modification (Lee et al., 2009; Marchionna et al., 2008). DME can also be used to produce LPG as an intermediate in the indirect synthesis of LPG.

Table 2.3 Properties of DME and LPG

Property	DME	Propane	Butane
Boiling point, °C at 1 atm	-24.9	-42.1	-0.5
Vapor pressure at 20°C, bar	5.1	8.4	3.1
Liquid density at 20°C, kg/m ³	668	501	610
Lower Heating Value, KJ/Kg liquid	28360	45990	45367
Lower/Upper flammability limit in air, vol.%	3.4-17	2.1-9.4	1.9-8.5

DME and Fuel Cell: Besides the direct methanol fuel cell (DMFC), in which the methanol reforming happens in the stack (internal reforming), direct DME fuel cell (DDMEFC) has been proposed with some advantages compared to DMFC. The energy losses due to fuel crossover in the DDMEFC are less than DMFC. DME also have higher energy density than methanol and close to ethanol (Cai et al., 2008). The data available about the DDMEFC is limited and the potential of this technology should be studied more.

DME as marine fuel: About 90 % of world trade is by ship, which has the lowest CO₂ emissions per ton per kilometer among other freight options. However, marine fuels are relatively high in sulfur which cause 4-6 % of SO_x to be produced by ships (Endresen et al., 2003). DME, as an excellent diesel fuel alternative, can be an option for diesel engine powered ships.

2.2.3. DME as intermediate

DME can be used as a chemical feedstock to many products such as short olefins (ethylene and propylene), gasoline, hydrogen, acetic acid and dimethyl sulfate. DME, using the LPG infrastructures for storage and distribution, can be easily transported to the areas far from oil and gas sources. It essentially behaves as liquid synthesis gas.

2.3. DME synthesis

DME can be produced from various raw materials as shown in Figure 2.1. DME synthesis, typically, involves the production of syngas, carbon monoxide and hydrogen, as a first step. The production efficiency depends on the sources available in the place of production. However, the wide variety of sources for syngas production makes it possible for all countries to contribute in DME production.

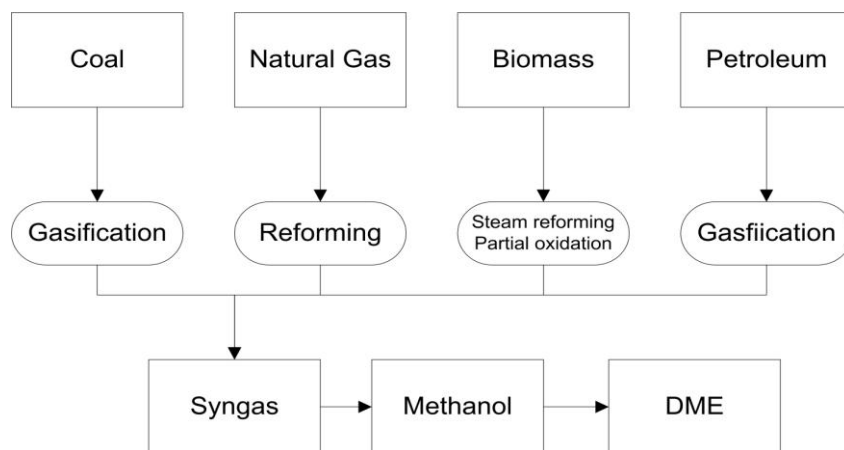


Figure 2.1 Different sources for DME synthesis

2.3.1. DME from synthesis gas

Commercially, natural gas is used to make the syngas. The procedure of using biomass and coal as raw materials for DME production includes more steps such as a gasification step to produce syngas. Some preparation processes for the biomass and coal are needed for more efficiency. Syngas produced from coal has a lower hydrogen to carbon ratio; therefore, it needs modification before using for methanol production to avoid formation of undesired by-products. On the other hand, some DME cleaning and purification procedures are needed for better product quality. Syngas synthesized from any source is converted to methanol according to following reactions (Equation (2.1) to (2.3)):



The first two reactions are exothermic and cause a decrease in volume. The reverse water-gas shift reaction is slightly endothermic. According to Le Chatelier's principle, the conversion into methanol is favored by decreasing temperature and increasing pressure. Today, the most widely used temperature and pressure range in methanol production is at 5-10 MPa and 250°C over a catalyst containing copper, zinc oxide and alumina, first used by Imperial

Chemical Industries (ICI) in 1966. Many studies have been made to improve the catalyst for methanol production (Meshkini et al., 2010; Zhang et al., 2006). Ma et al. (2008) determined higher sulfur tolerance in Pd/CeO₂ catalyst compared to Cu/ZnO and Pd/Al₂O₃. Methanol can be synthesized under mild reaction conditions (T=373 K, P=1.8 MPa) in a homogeneous Ni(CO)₄/KOME catalytic system (Li and Jiang, 1999).

DME is produced by the conventional bimolecular catalytic dehydration of methanol (Equation (2.4)) over various solid acids (Spivey 1991), such as alumina or phosphoric acid-modified γ -Al₂O₃ (Yaripour et al., 2005b)



2.3.2. Production processes

For industrial production, DME can be produced in liquid or gas phase catalyzed dehydration of methanol. Traditionally, strong mineral acids such as sulphuric acid, were used as catalyst, while in gas phase, solid acid catalysts are used. The liquid phase procedure involves high pressure and problems with catalyst separation, as the catalyst is homogeneous with reactants. Vapor phase process can be conducted to commercially acceptable conversions at temperatures around 300 °C. However, thermodynamically, at higher temperatures the equilibrium conversion decreases (Spivey, 1991) and methanol is converted to some other by-products (e.g. olefins) (Xu et al., 1997A).

DME can be produced from syngas using two methods, *indirect method* and *direct method*:

Indirect method: In the indirect method, syngas is converted to methanol with an appropriate catalyst; then, in another subsequent step, methanol, after being purified to be used for next step, is converted to DME over a solid-acid catalyst. In this method, methanol should be preheated before entering the fixed bed reactor where the vapor phase catalytic reaction takes place. Moreover, product separation, contaminant separation, separation of unreacted methanol and

recycling is needed for better product quality. In this method, two distillation columns are required for the separation procedure which makes it an energy intensive operation. Thus, the indirect method tends to be an expensive process.

Direct method: according to the fact that the conditions of the two consequent reactions are similar to each other; they can be conducted simultaneously in the same reactor over a bi-functional catalyst (Takeguchi et al., 2000; Sun et al., 2003; Xia et al., 2004; Ramos et al., 2005). This direct method, which is called syngas to dimethyl ether (STD) process was developed by Topsøe for DME synthesis from syngas (Top-Jorgensen, 1985). STD process is a single step vapor phase process where three reactions, namely water-gas shift reaction, methanol synthesis and methanol dehydration take place in a fixed bed reactor to exploit their potential synergy. This combination of reactions affects the methanol production equilibrium. Because the methanol produced in the first step is used in methanol dehydration reaction, there is more conversion in a single step of DME synthesis compared to the indirect method. The disadvantage of this process is that high operating conditions cause more by-product synthesis, which in return needs more complex distillation to separate the reactor effluent to achieve high purity DME.

Methanol synthesis from synthesis gas is thermodynamically unfavorable; thus, high pressure is required for the reaction (Kim et al., 2004), while the so called direct synthesis of DME from syngas over bi-functional catalysts seems to be thermodynamically more favorable (Li et al., 1996; Ge et al., 1998; Ng et al., 1999; Fei et al., 2006b). Recently, more focus is on methanol dehydration process and dimethyl ether purification. In the following section, the literature survey on the work concerning catalytic methanol dehydration for production of dimethyl ether will briefly be presented.

2.4. Catalytic methanol dehydration

The dehydration of alcohol is known to be an acid catalyzed reaction. A good catalyst for methanol dehydration reaction should work at as low a temperature as possible to minimize the heating time of catalyst and to avoid subsequent dehydration of DME to Olefins or hydrocarbons. A wide range of solid acid catalysts has been implemented for this reaction, with different purposes such as finding the optimum reaction condition, the most active and selective catalyst, kinetics information and so on. In the following section some of the major findings are discussed.

2.4.1. Solid-acid catalysts

Solid-acid catalysts play a crucial role in chemical industries as being used more in the production of organic chemicals. Solid-acid catalyst behavior can be categorized by their Brønsted and/or Lewis acidity, the strength and number of these sites and the morphology of the support i.e. surface area, pore size, etc. Solid-acids catalysts are used in solid-liquid and solid-gas reactions and can be easily separated from the reactants and products. The pore structure of these catalysts determines the accessibility of the active sites to diffusing reactant molecules. One important drawback of solid-acid catalysts is deactivation. They can be deactivated by H₂S, CO, Pb, As, Hg.

Dehydration of methanol to DME can be achieved by employing solid-acid catalysts such as γ -alumina, zeolite and ion exchange resins. These catalysts can be further modified to enhance their activity and performance for this particular reaction. The major preference is higher selectivity for DME formation and less deactivation of the catalyst. According to many studies on solid-acid catalysts, strong acidic sites produce unwanted by-products such as hydrocarbons (Spivey, 1991; Xu et al, 1997b). Both Brønsted and Lewis acid sites can catalyze the methanol DME reaction.

Although the acidity of the catalyst plays a crucial role in its performance, other factors such as thermal and mechanical stability, pore size and distribution as well as cost will determine the final choice.

γ -Alumina: Commercially, γ -alumina is used in DME synthesis through methanol dehydration. The catalytic activity of γ -alumina for methanol dehydration is linked to Lewis acid-Lewis base pair formed during calcination (Figoli et al., 1971). A mechanism involving an acid-base pair in methanol dehydration was proposed by Padmanabhan and Eastburn (1972) (Figure 2.2). However, Yaripour et al. (2005a) concluded that the hydration reaction takes place mainly on Brønsted acid sites. Fu et al. (2005) also suggested moderate strength surface Brønsted acid sites catalyze the stable conversion of methanol to DME.

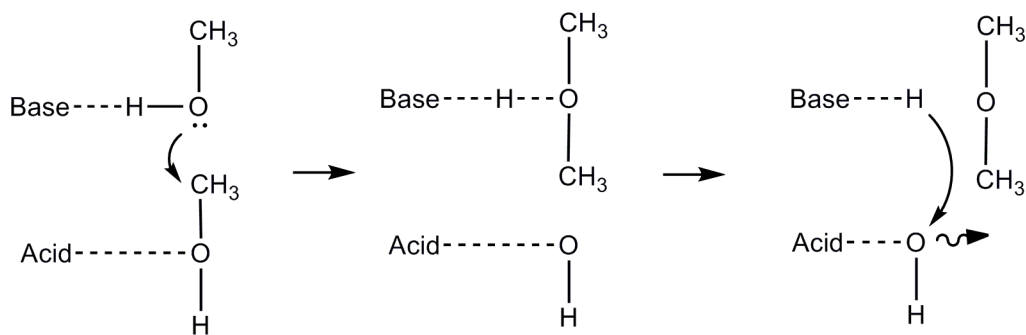


Figure 2.2 Bimolecular mechanism of methanol dehydration on an acid-base pair (Spivey,1991)

Yaripour et al. (2005b) observed good initial catalytic activity of γ -alumina for methanol dehydration at 300 °C and atmospheric pressure but slowly deactivated with time on stream. This activation is related to competition of water and methanol to capture the acid sites (Mollavali et al., 2008). Fu et al. (2005) also suggest water adsorption to Lewis acid sites as the reason of the catalyst deactivation.

The γ -alumina was modified with Si for better catalytic performance (Yaripour et al., 2005a). By modifying the alumina with silica, the surface acidity of aluminosilicate catalysts increased with increasing in silica loading. Fu et al. (2005) modified γ -alumina by Titania ($\text{Ti}(\text{SO}_4)_2$) to enhance the number and strength of surface Brønsted acid sites and thereby the dehydration activity. In addition, no detectable hydrocarbon or coke was formed over the modified γ -alumina with $\text{Ti}(\text{SO}_4)_2$. Using a series of commercial γ -alumina catalysts, Mollavali et al. (2008) determined acid sites with weak to moderate strength show higher activity and stability for this reaction. They found the selectivity of DME at lower temperatures around 100 %.

In general, γ -alumina is commercially preferred because of its fine particle size, high surface area, excellent thermal stability, high mechanical resistance and low cost catalyst (Mekasuwandumrong et al., 2003). But its hydrophilic property makes it deactivate quickly; therefore, it has been modified with fluorine, borate, silica, phosphorous, and titanium in order to improve its performance (Xia et al., 2006; Duarte et al., 2004; Yaripour et al., 2005a; Yaripour et al., 2005b; Fu et al., 2005).

Zeolites: Zeolite is another widely studied solid-acid catalyst for methanol dehydration to DME. Water has a smaller poisoning effect over zeolites such as ZSM-5 (Xu et al., 1997b) compared to γ -alumina. It has been reported that zeolite has more methanol conversion in lower temperatures. However, above the temperature of 270 °C side reactions such as olefin formation are auto catalytic over zeolite (Xu et al., 1997b). Generally, a binder material is added to zeolite catalysts to enhance the mechanical strength and stability of the catalyst. For instance, Kim et al. (2006) used γ -alumina as a binder to Na-modified ZSM-5, resulting in more stability against coke formation and water.

In STD process H-ZSM-5 besides $\text{Cu}/\text{ZnO}/\text{Al}_2\text{O}_3$ has been used a bi-functional catalyst for methanol dehydration (Haldor, 1993 a; Haldor, 1993b). H-ZSM-5 has both Lewis and Brønsted acid sites with dominant Brønsted site. Xu et al. (1997b) found activity for H-ZSM-5 as low temperature as 130 °C. Vishwanathan et al.

(2004a) found superior performance with Na modified ZSM-5, essentially eliminating catalyst strong surface acid-sites by partial substitution of Na in ZSM-5, for methanol dehydration at 230-340 °C.

Of particular interest for methanol dehydration, wide-pore zeolites (faujasites X and Y and Mordenite) have also been studied. Zeolite X is generally less hydrothermally stable than Y and has lower Si/Al ratio (Spivey, 1991). HY and Fe-, Co-, and Cr modified HY, which possess a higher proportion of strong acid sites, deactivate easily due to the carbon deposition. Zr and Ni-modified HY zeolites exhibit higher stability attributed to the lower proportion of strong acid sites on its surface (Fei et al., 2006a). Zeolite SUZ-4 has been found to be a very selective and stable catalyst in methanol dehydration to DME because the formed DME is not converted to hydrocarbons (Jiang et al., 2004).

Khandan et al (2008) tried a variety of Zeolites (i.e. ZSM-5, Y, Mordenite, Ferrierite and Beta) to find an optimum catalyst for methanol dehydration reaction at 250 °C and 30 bar. They indicate that methanol conversion and DME selectivity decreases as the Si/Al ratio is increased in the zeolites. The cation type is another important factor in DME synthesis whereas the exchange of sodium ion with hydrogen and ammonium causes enhancement in catalyst activity and selectivity. They found Al-modified HM zeolite as the most active, selective and stable zeolite for this reaction.

Ion exchange resin: Ion-exchange resins, fabricated from an organic substrate, are widely used in different separation, purification, and decontamination processes (e.g. water softening and purification). Ion-exchange resins were introduced as a more flexible substitute for natural or artificial zeolites in such applications. Typically, ion-exchange resins are based on crosslinked polystyrene by adding 0.5-25% of divinylbenzene to styrene at the polymerization process. The functional groups can be introduced after polymerization, or substituted monomers can be used. Non-crosslinked polymers are used rarely because they are less stable. More crosslink in the ion exchange resin decreases ion- exchange

capacity of the resin and prolongs the time needed to accomplish the ion exchange processes.

There are four functional groups used in Ion exchange resins: Strong acid (sulfonic group), strong basic (amino group), weakly acidic (carboxylic acid), and weakly basic (secondary or ternary amino groups). Amberlyst, which is Ion exchange resin made of crosslinked polystyrene with divinylbenzene, is the trademark of Rohm and Haas Company. This catalyst provides Brønsted acid sites for the dehydration reaction.

Amberlyst is a catalyst of great interest in methanol dehydration, as it requires a relatively low operating temperature (30-150 °C) and high selectivity to DME at this low temperature is achieved (Spivey, 1991; An et al., 2004). According to Gates and Johanson (1971), sulfonic functional groups are capable of DME production from methanol without the conjugate separate base site which is replaced by the hydroxyl groups associated with the sulfonic acid sites. Water effect on Amberlyst, same as other solid-acid catalysts, is significant because water competes with methanol for the acid site (An et al., 2004).

Other catalysts: other solid-acid catalysts have been investigated for this reaction. Moreno-Castilla et al. (2001) investigated oxidized activated carbon catalyst for methanol dehydration and determined that the activity of the catalyst is related to the H^+ concentration. Metal oxides and metal salts, other types of solid-acid catalysts, have also been implemented for this reaction. Vishwanthan et al. (2004b) tried a series of TiO_2 - ZrO_2 mixed oxides with various ratios at 280-340 °C and found good selectivity for temperatures below 300 °C. Sun et al. (2007) tried Nb_2O_5 and $NbOPO_4$ at 180-340 °C and compared them to ZSM-5 and γ -Alumina. The result shows the same activity as γ -Alumina for Nb_2O_5 and $NbOPO_4$, but very lower than ZSM-5. However, it had good selectivity to DME and stability against water.

2.4.2. Reaction kinetics

A number of researches on the kinetics of the synthesis of DME by dehydration of methanol on solid-acid catalysts have been published. Most of kinetic expressions were estimated at global scale, and only a few people tried to establish a detailed mechanism. Majority are in agreement that the catalytic methanol dehydration reaction mechanism follows either Langmuir - Hinshelwood (Gates and Johanson, 1971) or Eley-Rideal Kinetic models (Kiviranta-Paakkonen et al., 1998). Summary of some of published kinetic models for DME synthesis by catalytic dehydration of methanol is given in Table 2.4.

Most models presented in the literature show that water formed during the reaction inhibits the reaction. Most works have also demonstrated that the inhibition of the main product, dimethyl ether, is very small compared to water. In addition, Gogate et al. (1990) indicates that because of higher vapor pressure of DME compared to methanol and water, it can be postulated that the mol fraction of DME in the liquid-phase will be much less than that of either water or methanol. Hence, the extent of the reverse reaction is decrease and the equilibrium conversion is close to 100 %.

Table 2.4 Kinetic models studied for methanol dehydration to DME

	Reaction kinetic equation	Catalyst used	Reference
1.	$r_{DME} = \frac{kK_M^2 P_M^2}{(1 + K_M P_M + K_W P_W + K_D P_D)^2}$	Ion exchange resin	Gates and Johanson (1971)
2.	$r_{DME} = \frac{kK_M P_M^{\frac{1}{2}}}{1 + K_M P_M^{\frac{1}{2}} K_W P_W}$	γ -Al ₂ O ₃	Bercic and Levec (1992)
3.	$r_{DME} = \frac{kK_M^2 (P_M^2 - (P_W P_D / K_{eq}))}{(1 + 2\sqrt{K_M P_M} + K_W P_W)^4}$	γ -Al ₂ O ₃	Bercic and Levec (1992)
4.	$r_{DME} = \frac{(P_M^2 / P_W) - (P_D / K_{eq})}{(1 + K_M P_M + K_W P_W)^2}$	γ -Al ₂ O ₃	Lu et al. (2004)
5.	$r_{DME} = \frac{kK_M C_M^2}{(1 + K_M C_M + K_W C_W + K_D C_D)}$	Ion exchange resin	An et al. (2004)
6.	$r_{DME} = \frac{kP_M - (k / K_{eq})(P_D P_W / P_M)}{1 + K_M P_M + (P_W / K_W)}$	γ -Al ₂ O ₃	Mollavali et al. (2008)

There are a few studies that have proposed a detailed reaction mechanism for this reaction. For example, Lu et al. (2004) developed a detailed intrinsic mechanism containing seven elementary reactions. This mechanism was used by Mollavali et al., (2008) to derive kinetic global reaction equations as shown in Table 2.4. The two groups used different rate determining steps and arrived at different form rate equations.

In the mechanism introduced by Gates and Johanson (1969), shown in Figure 2.3, is assumed that two methanol molecules occupy two adjacent acid sites. The Langmuir-Hinshelwood (LH) model (Equation (2.5)) is used for this mechanism.

$$\text{Model 1 (LH)} \quad r_{\text{DME}} = \frac{k_S K_M^2 C_M^2}{(1 + K_M C_M + (K_W C_W)^n + K_D C_D)^2} \quad (2.5)$$

where k_S is the surface reaction rate constant, and K_M , K_W , and K_D , and C_M , C_W , and C_D are the adsorption equilibrium constants and concentration of methanol, water and DME, respectively, and n equals 0.5, 1 or 2.

On the other hand, in the Eley-Rideal (ER) model (Equation (2.6)) proposed by Kiviranta-Paakkonen (1998), only one methanol molecule adsorbs on the acid site which reacts with a second molecule from the liquid bulk phase (Figure 2.4) , and n equals 0.5, 1 or 2.

$$\text{Model 2 (ER)} \quad r_{\text{DME}} = \frac{k_S K_M^2 C_M^2}{(1 + K_M C_M + (K_W C_W)^n + K_D C_D)} \quad (2.6)$$

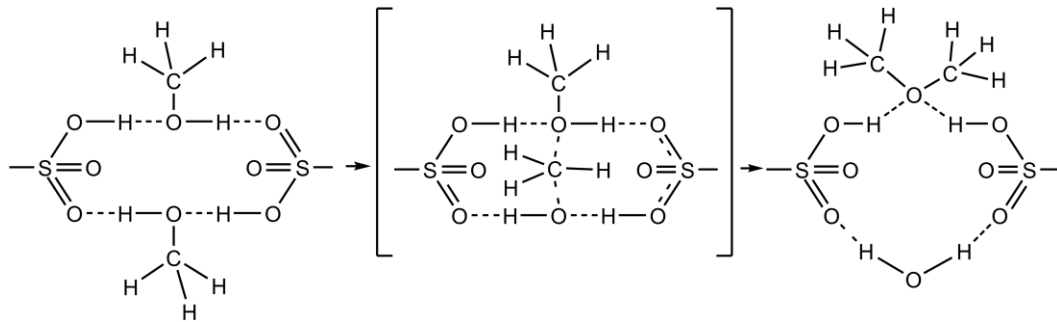


Figure 2.3 Gates and Johanson (1969) mechanism for methanol dehydration reaction

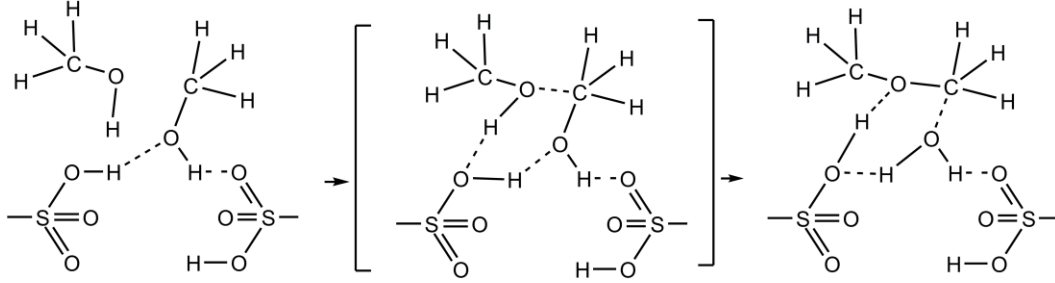


Figure 2.4 Kiviranta-Paakkonen (1998) mechanism for methanol dehydration reaction

2.5. Summary

As discussed in this chapter, different solid-acid catalysts show different types of behavior for the methanol dehydration reaction. Among these catalysts, γ -alumina and zeolites demonstrate proper activity but different selectivity to DME depending on their acid site strength. In this study, the activity of γ -alumina and the most active zeolites suggested by Khandan et al. (2008) i.e. ZSM-5 and Mordenite are investigated. Moreover, the activity of these catalysts is compared to four commercial ion exchange resins (i.e. Amberlyst 15, Amberlyst 35, Amberlyst 36 and Amberlyst 70). Then, a catalyst with favorable activity, selectivity and stability at the desired temperature and pressure will be selected for a more detailed kinetics study.

In the kinetics study, a set of experiments is conducted to find the best global model for the data. As investigated in many studies, the general form of the model selected for this work is

$$r_{\text{DME}} = \frac{k_S K_M^2 C_M^2}{(1 + K_M C_M + (K_W C_W)^n + K_D C_D)^m} \quad (2.7)$$

where k_S is the surface reaction rate constant, and K_M , K_W , and K_D , and C_M , C_W , and C_D are the adsorption equilibrium constants and concentration of methanol, water and DME, respectively, and $m = 1, 2$ and $n = 0.5, 1, 2$.

Equation (2.4) converts to Langmuir-Hinshelwood model (Equation (2.8)) by m equal to 2 and to Eley-Rideal (Equation (2.9)) by m equal to 1.

$$\text{Model 1 (LH)} \quad r_{\text{DME}} = \frac{k_S K_M^2 C_M^2}{(1 + K_M C_M + (K_W C_W)^n + K_{\text{DME}} C_{\text{DME}})^2} \quad (2.8)$$

$$\text{Model 2 (ER)} \quad r_{\text{DME}} = \frac{k_S K_M^2 C_M^2}{(1 + K_M C_M + (K_W C_W)^n + K_{\text{DME}} C_{\text{DME}})} \quad (2.9)$$

Chapter 3

Materials and Methods

This chapter contains a description of the experimental apparatus, the analytical instruments, the catalysts and other reagents, and all of the procedures used.

3.1. Catalysts and other Chemicals

The three liquids used as starting materials in the reactor were methanol, water and tetrahydrofuran. Research grade (99.9 %) methanol, the primary reactant, was obtained from Fisher Scientific. The water was obtained from a reverse osmosis system. With the reverse osmosis, about 99 % dissolved solids were removed from city water. Many experiments were carried out using methanol alone as the starting reagent. The effect of water was studied using binary mixtures of water and methanol. To study the effect of methanol concentration on the reaction rate, the initial methanol concentration was varied by the addition of an inert solvent. Initially, *o*-xylene was used; however, it was found that the ternary methanol/water/*o*-xylene samples gave two emulsion layers. It was concluded that to measure each reactant concentration would be neither reliable nor accurate. Therefore, it was decided to use tetrahydrofuran (THF) as the inert solvent. THF was obtained from Fisher Scientific.

The catalysts commonly used in the catalytic dehydration of methanol to DME are acid catalysts. Silica Alumina, γ -Alumina and different kinds of zeolites, namely, Mordenite, ZSM-5 and Y show good methanol conversion and selectivity to DME at high temperatures and pressure. However, catalytic distillation of DME takes place at relatively low pressure (8-12 bar) and temperatures in the range of 50-180 °C (Di Stanislao et al., 2007). It is not clear from the literature as to the best choice of catalyst, and therefore one of the objectives of this study was to determine the catalysts to use for this application. The final choice will have combination of strongest acidic strength and highest number of active sites and

resistance to water inhibition and side product formation. In this study, γ -alumina, three different zeolites having different acidity strength and finally, four different cation ion exchange resin Amberlyst catalysts were investigated.

Zeolites:

ZSM-5 and Mordenite, namely, CBV21, CBV8014 and CBV28014 were obtained from the Zeolyst International Company (USA). These catalysts have different $\text{SiO}_2/\text{Al}_2\text{O}_3$ ratios, which indicate different acidity strength. Increase in $\text{SiO}_2/\text{Al}_2\text{O}_3$ decreases the acidity strength but the amount of acidity remains almost the same (Khandan et al. 2008). The catalysts were calcined at 500 °C for 4 hours with heating rate of 6 °C/min from 25 to 500 °C. Table 3.1 shows the zeolites' properties, as provided by the Zeolyst Company.

Zeolites, as received, are in NH_4^+ form, which is inactive for methanol dehydration. They have to be calcined to convert the ammonium cations to hydrogen by removing the ammonia. Calcination is a process that catalyst is heated up to 400-500 °C and remains for a period of time as a carrier gas (He) flows in the furnace tube. Depending on the calcination procedure, the acid sites strength can be varied. We used Khandan et al. (2008) procedure for calcination of the Zeolites. The released ammonia is directed to vent after passing through HCl solution. A Thermolyne 79400 tube furnace was used for the calcination process. The calcined zeolite adsorbs moisture of the air very rapidly; thus, it should be moved to a vacuum chamber quickly after removed from the furnace.

Table 3.1 Properties of three different Zeolites catalysts

Zeolyst Product	Zeolite	$\text{SiO}_2/\text{Al}_2\text{O}_3$ Mole ratio:	Nominal Cation Form	Surface area m^2/g
CBV 28014	ZSM-5	280	Ammonium	400
CBV 8014	ZSM-5	80	Ammonium	425
CBV 21	Mordenite	20	Ammonium	500

Amberlyst:

Amberlyst 15, 35, 36 and 70 were obtained from Rohm and Haas Company (USA). They were received in wet form with water. They were dried prior to use using a vacuum dryer to remove the adsorbed water. Amberlyst series catalysts' properties are shown in Table 3.2, which were provided by the company.

Table 3.2 Amberlyst series catalysts properties

Name	Amberlyst 15	Amberlyst 35	Amberlyst 36	Amberlyst 70
Acidity (Eq/kg) ¹	4.6	5.13	5.38	2.7
Surface area (m ² /g):	53	50	33	36
Average pore diameter (Å):	300	300	240	220
Mean size (mm)	0.6 -0.85	0.7-0.95	0.6-0.85	0.5
Pore volume (ml/g):	0.4	0.35	0.2	NA
Swelling (water to dry)	37	40	54	NA
Operating Temperature limit	120	150	150	190

¹. Calculated by Rohm and Haas Co. procedure (Appendix C)

3.2. Vacuum Dryer

To remove water from the catalysts, a vacuum dryer was used. The catalyst was placed in a glass chamber, and temperature was controlled with a PID controller. Nitrogen, as inert gas, was flowing over the catalyst to the vacuum all the time of drying to carry out the water. To prevent the system from overshooting, using ramp and soak controlling method, first, the temperature was increased to 95 °C,

where it was held for 1 h; then increased to 110 °C where it was held for 8 hours. The pressure was set to 635 Torr absolute using a vacuum pump. The nitrogen flows at a rate of 100 SCCM controlled by a Matheson 8200 mass flow controller. Figure 3.1 shows the diagram of the vacuum dryer set-up.

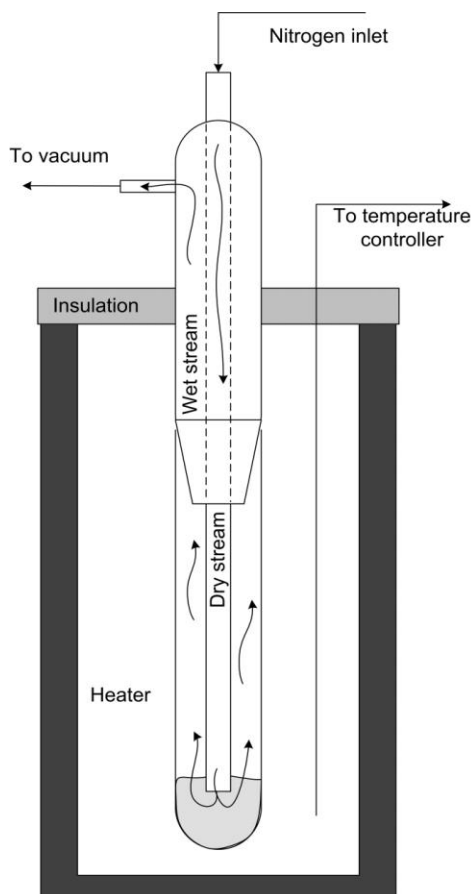


Figure 3.1 The vacuum dryer used to remove water from the catalyst samples.

3.3. Reactor

The reactions were carried out in a 480 cm³ batch autoclave equipped with a stirrer (four blade glass impeller) and a heating jacket. A diagram of the reactor is given in Figure 3.2. The body of the reactor is made of 316 stainless steel. The temperature of the reactor is controlled using Parr 4841 proportional controller. The stirrer was connected to a variable speed motor and the speed was calibrated using a Tachometer. The bearing of the stirrer was cooled by water circulation.

The operating temperature and pressure limits for the autoclave are 400 °C and 200 bar. A rupture disc prevented the pressure from exceeding 140 bar. A J-type thermocouple was used to measure the temperature. The liquid was sampled via a 1/16" diameter tube equipped with a sintered 316 stainless steel metal filter with pore size of approximately 300 Mesh to prevent it from being plugged by catalyst. A Swagelok needle valve was used to control the flow rate of liquid. Another Swagelok needle valve was used on a gas vent to collect the vapor. A double pipe heat exchanger (condenser) of 0.3 m length was connected to the gas vent to prevent methanol and water vapors escaping through gas vent during gas sampling. For safety matters, the experiments were carried out in appropriate ventilation conditions. The heat exchanger was connected to a circulating bath water cooler. The coolant was aqueous antifreeze solution.

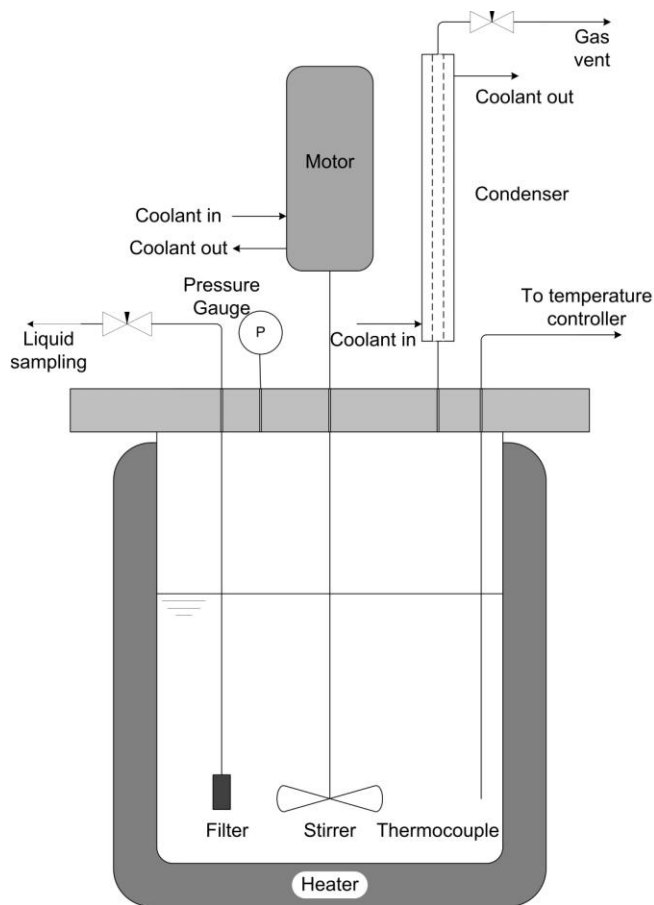


Figure 3.2 Schematic of the batch reactor used in this study

3.4. Sample analysis

The liquid samples were analyzed using a Hewlett-Packard 5710A series gas chromatograph (GC) equipped with a thermal conductivity detector (TCD) and an HP 3392 integrator. The 10 feet long and 1/16" diameter column, used in GC was a Supelco Co. stainless steel HayeSep D column with mesh 80/100. Ultra high pure helium is used as the carrier gas with the flow rate of 35 ml/min. The detector and injection port temperatures are set to 200 °C and 250 °C respectively with auxiliary temperature off. The oven temperature is set constant at 165 °C with attenuation and sensitivity at 4.

The GC was calibrated for binary methanol-water mixtures. For binary mixture, the liquid samples with known concentrations were prepared in the range of changes of the reaction. These liquid samples were prepared by mixing deionized water with research grade methanol obtained from Fisher Scientific. Each known sample was then injected four times to estimate the error of measurements. Table 3.3 shows the GC responses expressed as area percent of methanol versus known weight percent of methanol as well as the standard deviations.

The relationship between known weight percent of methanol and area percent of methanol is shown in Figure 3.3. The calibration to determine the weight percent of the methanol for methanol/water mixture was obtained using a nonlinear regression in following form:

$$\text{Wt \% of methanol} = 0.001832(\text{Area}\%)^3 - 0.4993(\text{Area}\%)^2 + 46.3(\text{Area}\%) - 1369$$

Table 3.3 Area percent of methanol and known weight percent of methanol

GC. Response (Area % of methanol)	Known % methanol (Wt %)	Standard Error 95% confidence
99.25	98.99	0.03
98.40	97.96	0.02
97.61	97.00	0.08
95.98	95.01	0.07
93.03	91.99	0.08
90.87	89.99	0.08
87.87	87.00	0.1
85.91	85.00	0.08

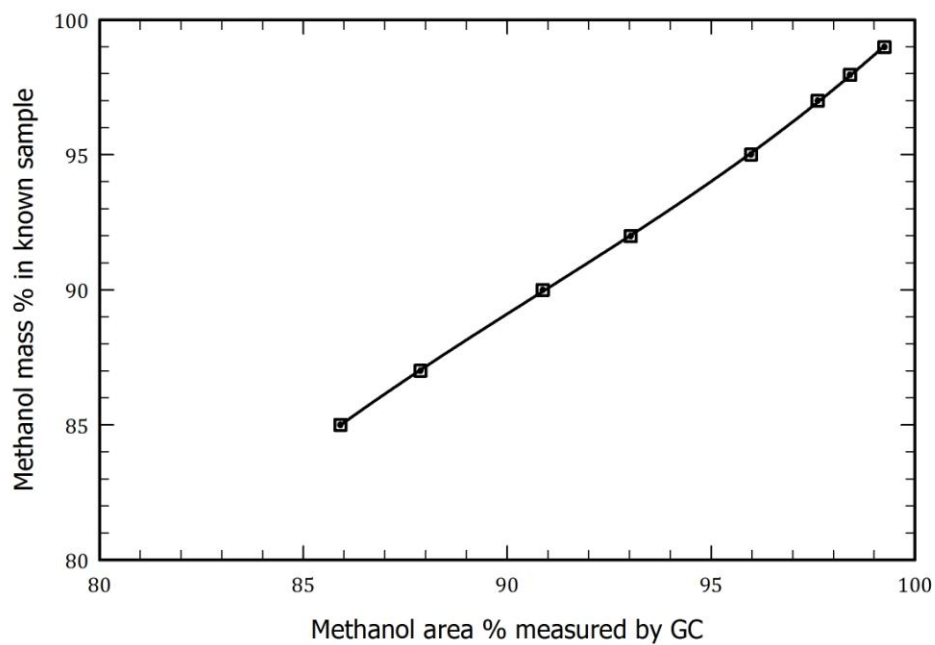


Figure 3.3 GC calibration curve for methanol-water solutions

The GC was again calibrated using ternary methanol/water/tetrahydrofuran mixtures in the range of changes of the reaction. In the ternary mixtures, the amount of tetrahydrofuran was varied from 33 % to 83 % by weight. These liquid samples were prepared by mixing deionized water with research grade methanol and tetrahydrofuran obtained from Fisher Scientific. Each known liquid sample was then injected four times to minimize the error of measurements. The relationship between known weight percent of methanol and are percent of methanol for three different tetrahydrofuran concentrations is shown in Figure 3.4. For this ternary system, the calibration equations to determine the weight percent of the methanol was obtained using a nonlinear regression for three different tetrahydrofuran concentrations are shown in Table 3.4.

Table 3.4 The GC calibration for three tetrahydrofuran concentrations

THF (Wt %)	Calibration equations	R ²
33	$Wt \% = 0.00211(\text{Area}\%)^3 - 0.5767(\text{Area}\%)^2 + 53.52(\text{Area}\%) - 1595$	0.998
50	$Wt \% = -0.000706(\text{Area}\%)^3 + 0.2063(\text{Area}\%)^2 - 18.85(\text{Area}\%) + 628$	0.998
67	$Wt \% = 0.0001366(\text{Area}\%)^3 - 0.01969(\text{Area}\%)^2 + 1.353(\text{Area}\%) + 25.56$	0.999
83	$Wt \% = -0.0001566(\text{Area}\%)^3 + 0.04048(\text{Area}\%)^2 - 2.346(\text{Area}\%) + 86.96$	0.998

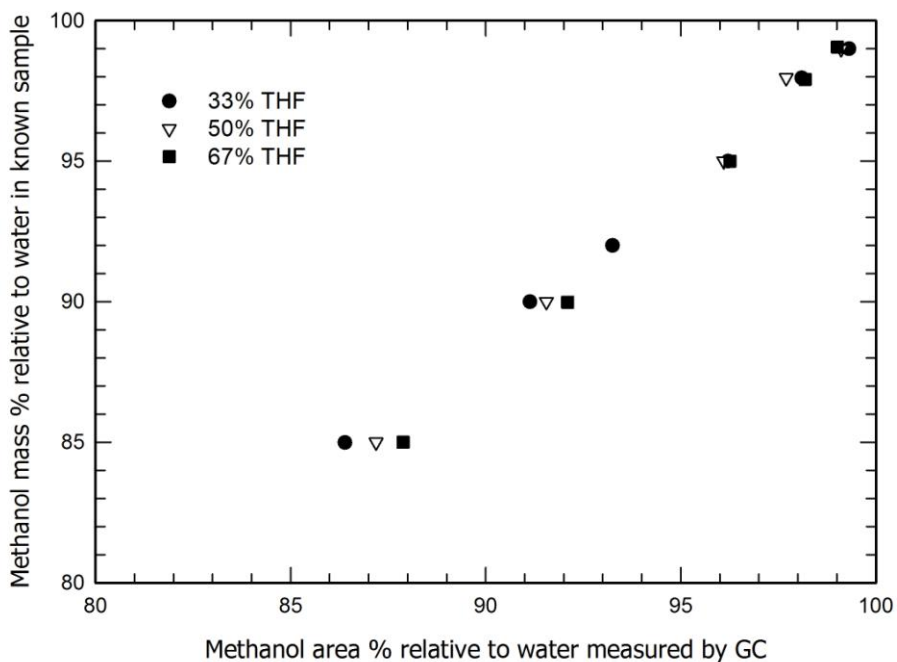


Figure 3.4 GC calibration curves for methanol-water-THF solutions

A Hewlett-Packard 5970 series GC/MS equipped with a DB-5MS capillary column with 30 m in length and 0.25 mm in diameter was used to determine if the liquid samples contained any byproduct other than that DME. This GC was able to detect product with molecular weight of 15 - 550. For this analysis, the injector and detector temperatures were set to 280 °C. The oven temperature is kept constant at 35 °C for 5 minutes and then increased to 280 °C at a rate of 10°C/min. 1 µL of liquid sample was injected with a split ratio is 100:1 and gas sample injection is splitless 10 µL of sample. The result of the GC-MS analysis shows that there is no detectable by-product produced at this operating condition.

3.5. Acidity Determination

The acidity of the catalyst was measured according to the procedure suggested by Rohm and Haas Co. We used one tenth of the values suggested by the procedure. For instance, 1.5 g of each Amberlyst is ion exchanged with 100 cm³ of sodium

nitrate and 100 cm³ of HCl in regeneration. The procedure includes passing sodium nitrate through the catalyst bed where the cation exchange happens. After exchanging the hydrogen ions in catalyst with sodium, the Catalysts is washed and regenerated by HCl to ion exchange the sodium ions by hydrogen. The regenerated catalyst is again ion exchanged by sodium nitrate, and exact 100 cm³ of solution is collected, and titrated by standard NaOH solution. The average of titration values is used for the calculation of acidity of Amberlyst.

3.6. Experimental Procedure

For each run, 120 ± 0.2 g of reactants (i.e. methanol, methanol/water or methanol/water/tetrahydrofuran mixtures) and 4 ± 0.001 g of catalyst were charged to the reactor. In some runs 8 ± 0.01 g of catalyst was used. The reactor was flushed several times with nitrogen and then pressurized to 900 ± 50 kPa. The reactor temperature was increased to a selected temperature in the range of 105-135 ± 1 °C. The reaction was induced by turning on the stirrer. The stirrer speed was set to 750 rpm in all tests to eliminate the effect of external mass transfer on the rate of reaction. After the reactants reached to the desired temperature and pressure, the liquid phase samples were taken at the times of 0, 30, 60, 120, 210 minutes and analyzed. For each time period, two separate liquid samples were taken. Each liquid sample was then injected four times to minimize the error of measurements.

3.6.1. Calculations

The liquid samples were analyzed and the weight fractions of methanol and water were obtained using the appropriate GC calibration equation. The total (i.e. cumulative) mass of dimethyl ether (DME) formed at the end of each time period was then calculated from a mass balance, based on the composition of the liquid samples. The procedure followed for a starting composition of pure methanol is

shown below. It was modified appropriately when the starting liquid was not pure methanol.

After charging the reactor with methanol and bringing the reactor operating temperature, the amount of liquid and gaseous methanol was estimated using a vapor liquid equilibrium calculation. The mass of this initial liquid feed is denoted as W_0 . As the reaction proceeds, methanol reacts to form DME and water. We assume that the DME goes to the gas phase and that the water stays in the liquid phase. This assumption is reasonable, because conversions were relatively low, and the majority of the water would remain in the liquid. The mass of produced water in the reactor at any point can be calculated by:

$$W_{\text{H}_2\text{O}} = w_{\text{H}_2\text{O}} W_i \quad (3.1)$$

where $w_{\text{H}_2\text{O}}$ is the measured mass fraction of the water in the liquid sample at time t , and W_i is the mass of the liquid in the reactor at that time. The number of moles of water is then:

$$N_{\text{H}_2\text{O}} = \frac{w_{\text{H}_2\text{O}} W_i}{M_{\text{H}_2\text{O}}} \quad (3.2)$$

where $M_{\text{H}_2\text{O}}$ is the molecular weight of the water. Methanol dehydration to DME produces the same number of moles of water and DME. The mass of DME can thus be calculated by:

$$W_{\text{DME}} = w_{\text{H}_2\text{O}} W_i \frac{M_{\text{DME}}}{M_{\text{H}_2\text{O}}} \quad (3.3)$$

As all of the DME is assumed to migrate to the vapor, the mass of the liquid in the reactor, W_i at time t can be calculated by the difference between the initial mass of the liquid and the mass of DME produced.

$$W_i = W_0 - W_{\text{DME}} \quad (3.4)$$

Equations (3.3) and Equation (3.4) represent a linear system of two equations with two unknowns. Combining and rearranging gives the mass of the liquid in the reactor at time t .

$$W_i = \frac{W_0}{1 + w_{\text{H}_2\text{O}} \left(\frac{M_{\text{DME}}}{M_{\text{H}_2\text{O}}} \right)} \quad (3.5)$$

The total mass of produced DME for each time period can be calculated by substituting Equation (3.5) into (3.3) to give:

$$W_{\text{DME}} = \frac{w_{\text{H}_2\text{O}} W_0 \left(\frac{M_{\text{DME}}}{M_{\text{H}_2\text{O}}} \right)}{\left[1 + w_{\text{H}_2\text{O}} \left(\frac{M_{\text{DME}}}{M_{\text{H}_2\text{O}}} \right) \right]} \quad (3.6)$$

The moles of DME produced per gram of catalysts (N_{DME}) can be calculated by

$$N_{\text{DME}} = \frac{W_{\text{DME}}}{W_{\text{cat}} \cdot M_{\text{DME}}} \quad (3.7)$$

To obtain the initial rate of the reaction at the any operating conditions, a second degree polynomial regression was used between the relationship of moles of DME produced per g of catalyst and time. The regression was forced through the origin and the initial rate of the reaction was obtained from the slope the regression line at time 0.

In experiments using THF diluted methanol solutions as the feed to the autoclave, the mass of methanol in the feed is used as the value of W_0 .

For experiments using water-methanol solutions as the feed to the autoclave, the total mass of produced DME for each time period can be calculated by

$$W_{\text{DME}} = \frac{W_0 \left(\frac{M_{\text{DME}}}{M_{\text{H}_2\text{O}}} \right) \left(w_{\text{H}_2\text{O}} + w_{\text{H}_2\text{O}} w_{\text{H}_2\text{O}_{\text{initial}}} \left(\frac{M_{\text{DME}}}{M_{\text{H}_2\text{O}}} \right) - w_{\text{H}_2\text{O}_{\text{initial}}} \right)}{\left[1 + w_{\text{H}_2\text{O}} \left(\frac{M_{\text{DME}}}{M_{\text{H}_2\text{O}}} \right) \right]} \quad (3.8)$$

Moreover, the methanol conversion can be calculated using the following equation

$$\text{Methanol conversion} = 100 \times \frac{W_0(1 - w_{\text{H}_2\text{O}_{initial}}) - W_i(1 - w_{\text{H}_2\text{O}})}{W_0(1 - w_{\text{H}_2\text{O}_{initial}})} \quad (3.9)$$

3.6.2. Error Analysis

The uncertainty for the initial reaction rate and the methanol conversion were calculated using the method described by Kline and McClintock (1953) and Holman (1984). The calculated initial reaction rate, R is a given function of the independent variables of $x_1, x_2, x_3, \dots, x_n$. Let u_R be the error in calculated initial rate and $u_1, u_2, u_3, \dots, u_n$ be the error in the independent variables. Then error in the initial reaction rate value can be calculated by

$$u_R = \left[\left(\frac{\partial R}{\partial x_1} u_1 \right)^2 + \left(\frac{\partial R}{\partial x_2} u_2 \right)^2 + \dots + \left(\frac{\partial R}{\partial x_n} u_n \right)^2 \right]^{0.5} \quad (3.10)$$

For present study the error in the DME moles produced in each time step (t) of the reaction was estimated by

$$u_{W_{\text{DME}}(t)} = \left[\left(\frac{\partial W_{\text{DME}}}{\partial W_0} u_{W_0} \right)^2 + \left(\frac{\partial W_{\text{DME}}}{\partial w_{\text{H}_2\text{O}}} u_{w_{\text{H}_2\text{O}}} \right)^2 \right]^{0.5} \quad (3.11)$$

Where u_{W_0} is the uncertainty in the initial amount of feed, and $u_{w_{\text{H}_2\text{O}}}$ is the uncertainty of the GC measurements for the water mass fraction, and can be calculated by (Montgomery and Runger, 2007)

$$u_{w_{\text{H}_2\text{O}}} = t_{\alpha, n-1} \frac{S_X}{\sqrt{n}} \quad (3.12)$$

S_X is the standard deviation of injection values, n is the number of injection for a sample, and $t_{\alpha, n-1}$ is the general t distribution with level of significance of α (i.e. 0.05) and degree of freedom of $n-1$.

By substituting the derivatives of Equation (3.6) in Equation (3.11) we derive to

$$\mathbf{u}_{W_{DME}(t)} = \left[\left(\frac{w_{H_2O} \left(\frac{M_{DME}}{M_{H_2O}} \right)}{\left[1 + w_{H_2O} \left(\frac{M_{DME}}{M_{H_2O}} \right) \right]} \mathbf{u}_{W_0} \right)^2 + \left(\frac{W_0 \left(\frac{M_{DME}}{M_{H_2O}} \right)^2}{\left[1 + w_{H_2O} \left(\frac{M_{DME}}{M_{H_2O}} \right) \right]^2} \mathbf{u}_{W_{H_2O}} \right)^2 \right]^{0.5} \quad (3.13)$$

For experiments using water-methanol solutions as the feed to the autoclave, the error for the mass of produced DME for each time period (Equation (3.8)) was calculated by

$$\mathbf{u}_{W_{DME}(t)} = \left[\left(\frac{\partial W_{DME}}{\partial W_0} \mathbf{u}_{W_0} \right)^2 + \left(\frac{\partial W_{DME}}{\partial w_{H_2O initial}} \mathbf{u}_{W_{H_2O}} \right)^2 + \left(\frac{\partial W_{DME}}{\partial w_{H_2O}} \mathbf{u}_{W_{H_2O initial}} \right)^2 \right]^{0.5} \quad (3.14)$$

and

$$\frac{\partial W_{DME}}{\partial W_0} = \frac{\left(\frac{M_{DME}}{M_{H_2O}} \right) \left(w_{H_2O} + w_{H_2O} w_{H_2O initial} \left(\frac{M_{DME}}{M_{H_2O}} \right) - w_{H_2O initial} \right)}{\left[1 + w_{H_2O} \left(\frac{M_{DME}}{M_{H_2O}} \right) \right]} \quad (3.15)$$

$$\frac{\partial W_{DME}}{\partial w_{H_2O}} = \frac{W_0 \left(\frac{M_{DME}}{M_{H_2O}} \right) \left(1 + 2 \left(\frac{M_{DME}}{M_{H_2O}} \right) w_{H_2O initial} \right)}{\left[1 + w_{H_2O} \left(\frac{M_{DME}}{M_{H_2O}} \right) \right]^2} \quad (3.16)$$

$$\frac{\partial W_{DME}}{\partial w_{H_2O initial}} = \frac{W_0 \left(\frac{M_{DME}}{M_{H_2O}} \right) \left(w_{H_2O} \left(\frac{M_{DME}}{M_{H_2O}} \right) - 1 \right)}{\left[1 + w_{H_2O} \left(\frac{M_{DME}}{M_{H_2O}} \right) \right]} \quad (3.17)$$

The error for methanol conversion (Equation (3.9)) was calculated using the following equation

$$\mathbf{u}_{\text{Methanol conversion}} = 10 \times \left[\left(\frac{(1-w_{H_2O})}{W_0(1-w_{H_2O initial})} \mathbf{u}_{W_i} \right)^2 + \left(\frac{W_i}{W_0(1-w_{H_2O initial})} \mathbf{u}_{w_{H_2O}} \right)^2 + \left(\frac{W_i(1-w_{H_2O})}{W_0^2(1-w_{H_2O initial})} \mathbf{u}_{W_0} \right)^2 + \left(\frac{W_i(1-w_{H_2O})}{W_0(1-w_{H_2O initial})^2} \mathbf{u}_{w_{H_2O initial}} \right)^2 \right]^{0.5} \quad (3.18)$$

The error for initial reaction rate (r_0) at any operation condition was calculated using the Holman method as described before. Substituting derivatives for r_0 in the Equation (3.10) we derive to

$$u_{r_0} = \left[\left(\frac{\partial r_0}{\partial W_{\text{DME}}(0\text{min})} u_{W_{\text{DME}}(0\text{min})} \right)^2 + \left(\frac{\partial r_0}{\partial W_{\text{DME}}(30\text{min})} u_{W_{\text{DME}}(30\text{min})} \right)^2 + \dots \right. \\ \left. + \left(\frac{\partial r_0}{\partial W_{\text{DME}}(210\text{min})} u_{W_{\text{DME}}(210\text{min})} \right)^2 \right]^{0.5} \quad (3.19)$$

the derivatives of initial reaction rates in Equation (3.19) was calculated by the following definition of derivation

$$\frac{\partial r_0}{\partial W_{\text{DME}}(t)} = \frac{r_{(W_{\text{DME}}(t)+\Delta W_{\text{DME}})} - r_{(W_{\text{DME}}(t))}}{\Delta W_{\text{DME}}} \quad (3.20)$$

The final experimental error for initial reaction rate in present study varies in the range of 2-8.5 %.

Chapter 4

Results and Discussion

Acidic catalysts are active for the dehydration of methanol. According to the previous studies, γ -alumina and zeolites are favorable catalysts at high temperatures. Ion exchange resins, on the other hand, have high cation exchange capacity, but they cannot be used at high temperatures because of their polymeric temperature-sensitive structure. However, at their operating temperature limit, they show significant activity for a variety of etherification, esterification and isomerization reactions. The optimal choice for catalyst will have the combination of strongest acidic strength and highest number of active sites, combined with a resistance to water inhibition and side product formation. Furthermore, we will also find a heterogeneous catalyst for the methanol dehydration reaction at moderate temperature and pressure.

In the present study, commercial solid-acids, such as γ -Alumina, Zeolites (Y, ZSM-5 and Mordenite) and ion exchange resins (Amberlyst 15, Amberlyst 35, Amberlyst 36, Amberlyst 70 and Amberlite IR-120) were investigated. For all of the above commercial solid-acid catalysts, methanol dehydration reaction is conducted below the maximum operational temperature at 110 ± 1 °C. For each run, 4 ± 0.005 g catalyst and 120 ± 0.2 g solution were charged into the reactor. The reactor was run for 3.5 hours and the DME synthesis rate and methanol conversion of the reaction were compared. It was found that γ -alumina and zeolites (Y) and Amberlite IR-120 did not have any detectible conversion of methanol. ZSM-5 and Mordenite on the other hand showed less than 3% methanol conversion at 130 °C.

ZSM-5, HM and Amberlyst 70 were also tested at higher temperature (150 °C) and pressure (1.7 MPa). The DME moles produced per gram catalyst and methanol conversion as a function of reaction time is shown in Figure 4.1 and 4.2 respectively. The amount of DME produced per gram of catalyst and methanol conversions were calculated using Equations (3.7) and (3.9), respectively. It can

be seen that Mordenite have about half of activity of the Amberlyst 70. Although both catalysts showed some methanol conversion, the reaction temperature and pressure were higher than those desired.

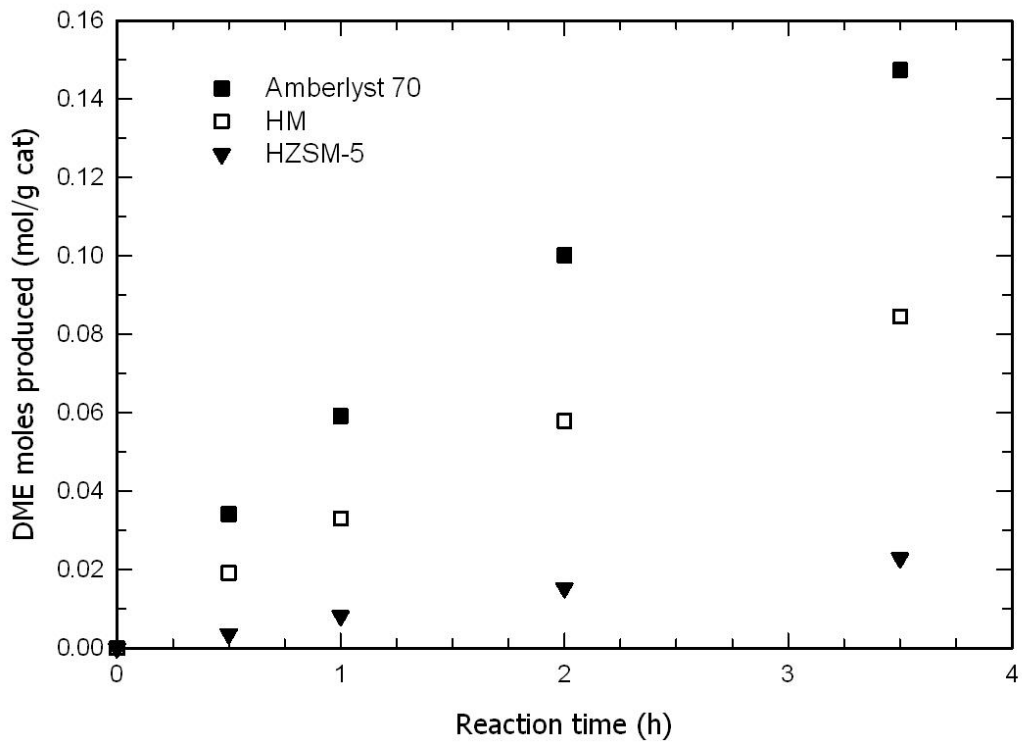


Figure 4.1 DME moles produced over Amberlyst 70 and H-ZSM-5 at 150 °C and 1.7 MPa

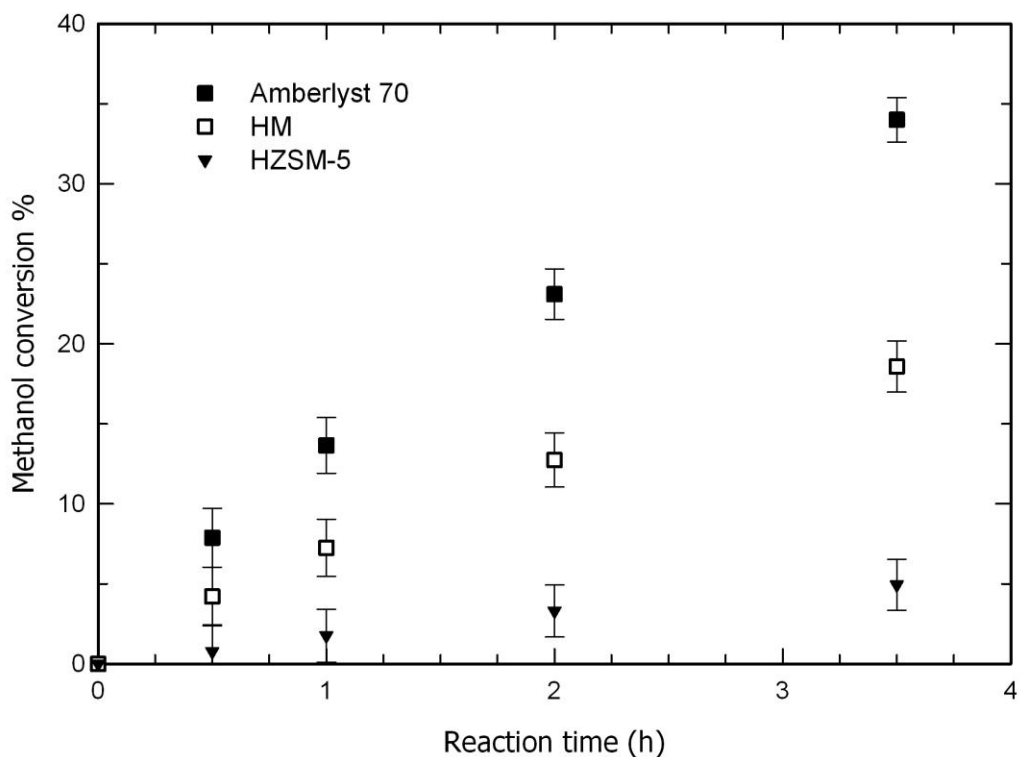


Figure 4.2 Methanol conversion over Amberlyst 70 and H-ZSM-5 at 150 °C and 1.7 MPa

Ion exchange resin catalysts have are active at mild operating conditions. Amberlyst 15, Amberlyst 35, Amberlyst 36, Amberlyst 70 catalyst performance was studied at moderate temperature (110 °C) and pressure (900 kPa) for 8 hours. Figure 4.3 shows the DME produced per gram catalyst while Figure 4.4 show methanol conversion as a function of reaction time for four Amberlyst catalysts. Both figures show that the DME production and methanol conversion for Amberlyst 35 and 36 are higher than Amberlyst 15 and 70. This was expected because both Amberlyst 35 and 36 have higher acidity than that Amberlyst 15 and 70, as shown in Table 3.2.

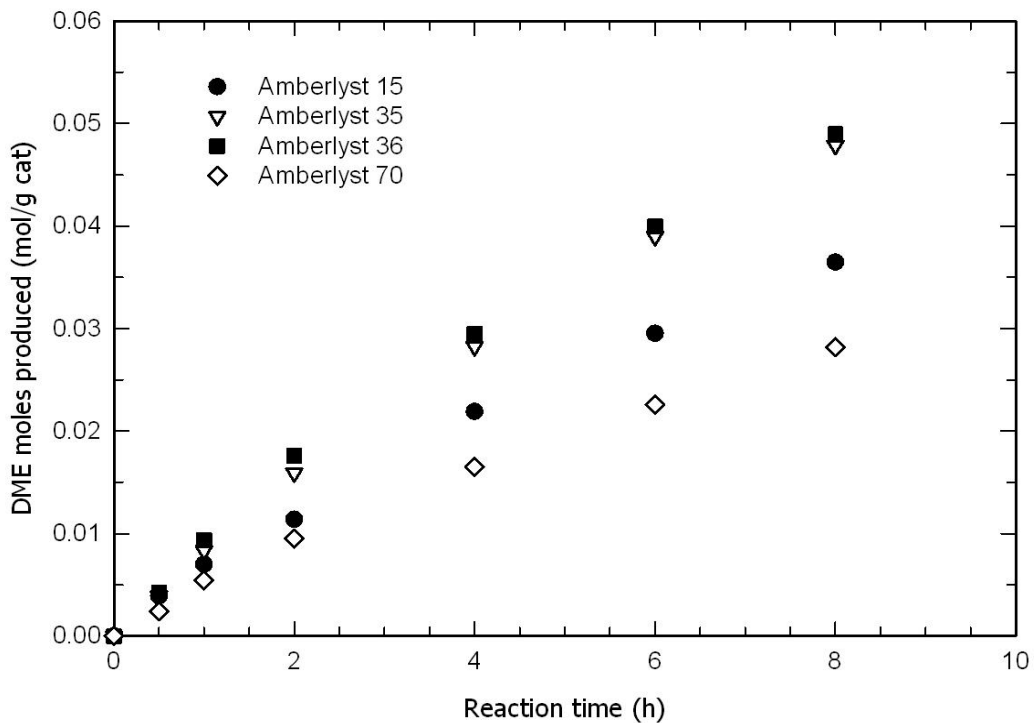


Figure 4.3 DME moles produced over Amberlyst 15, Amberlyst 35, Amberlyst 36 and Amberlyst 70 at 110 °C and 900 kPa using pure methanol as feed

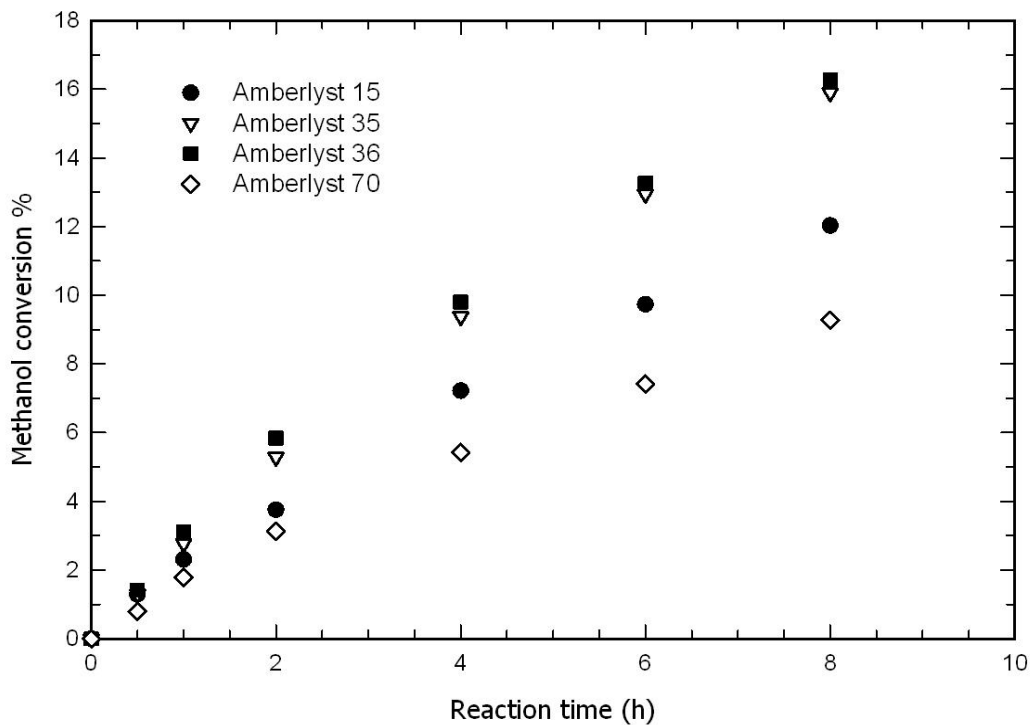


Figure 4.4 Methanol conversion over Amberlyst 15 Amberlyst 35 (Amberlyst 36 and Amberlyst 70 at 110 °C and 900 kPa using pure methanol as feed

The dehydration of methanol over Amberlyst 15, Amberlyst 35, Amberlyst 36 and Amberlyst 70 at 130 °C and pressure of 900 kPa was also carried out to examine the effect of temperature on performance of these catalysts. Figure 4.5 illustrates that both Amberlyst 35 and 36 have more activity than Amberlyst 15 and 70.

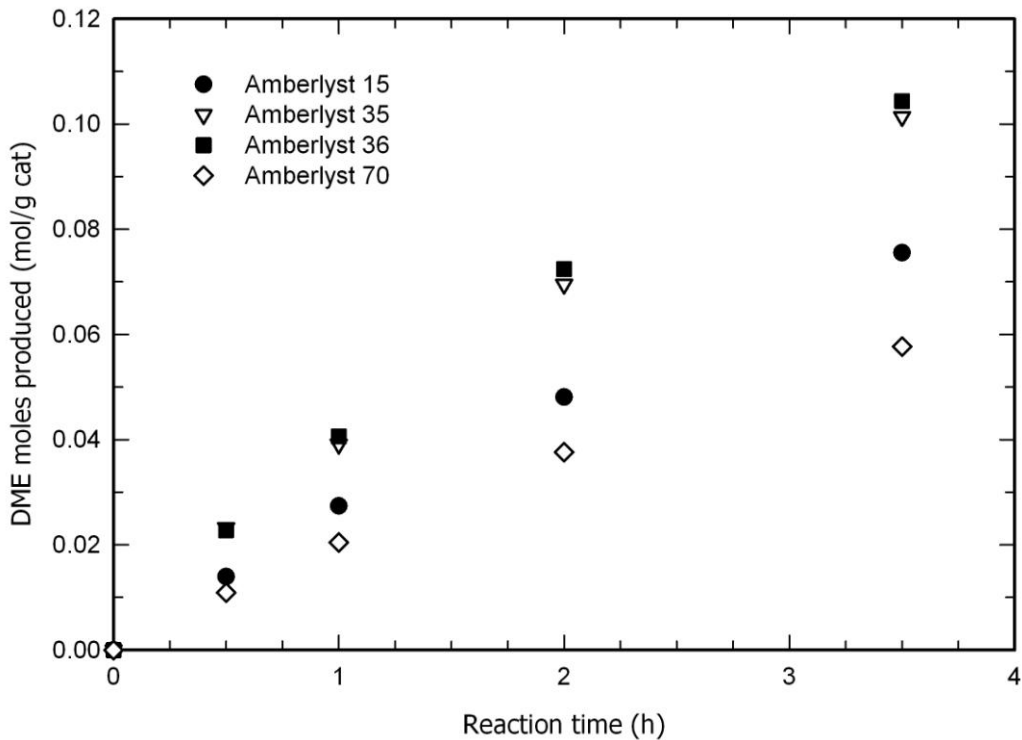


Figure 4.5 DME moles produced over Amberlyst 15 Amberlyst 35 Amberlyst 36 and Amberlyst 70 at 130 °C and 900 kPa using pure methanol as feed

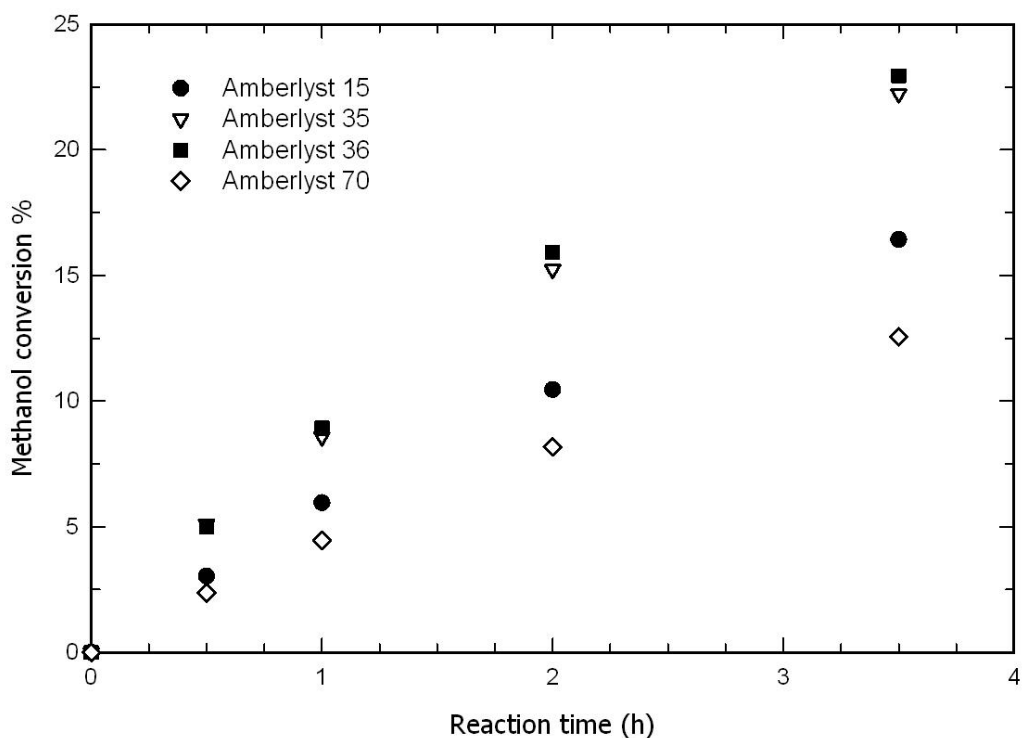


Figure 4.6 Methanol conversion over Amberlyst 15 Amberlyst 35 Amberlyst 36 and Amberlyst 70 at 130 °C and 900 kPa using pure methanol as feed

Water inhibits catalytic methanol dehydration to DME over either solid-acids or ion exchange resins. Water and methanol molecules compete for adsorption at catalytic active sites on the surface of acid catalyst. Figure 4.7 and Figure 4.8 show the reaction over Amberlysts 15, 35, 36 and 70 at 130 °C and pressure of 900 kPa for the initial water concentrations of 2.5 M and 3.5 M in methanol, respectively. Both figures shows that Amberlyst 35 and Amberlyst 36 have the same activity and much higher than Amberlyst 15 and 70. The comparison of two figures also indicates that the amount of the DME formation slightly decreased by increasing the initial water concentration from 2.5 M to 3.5 M.

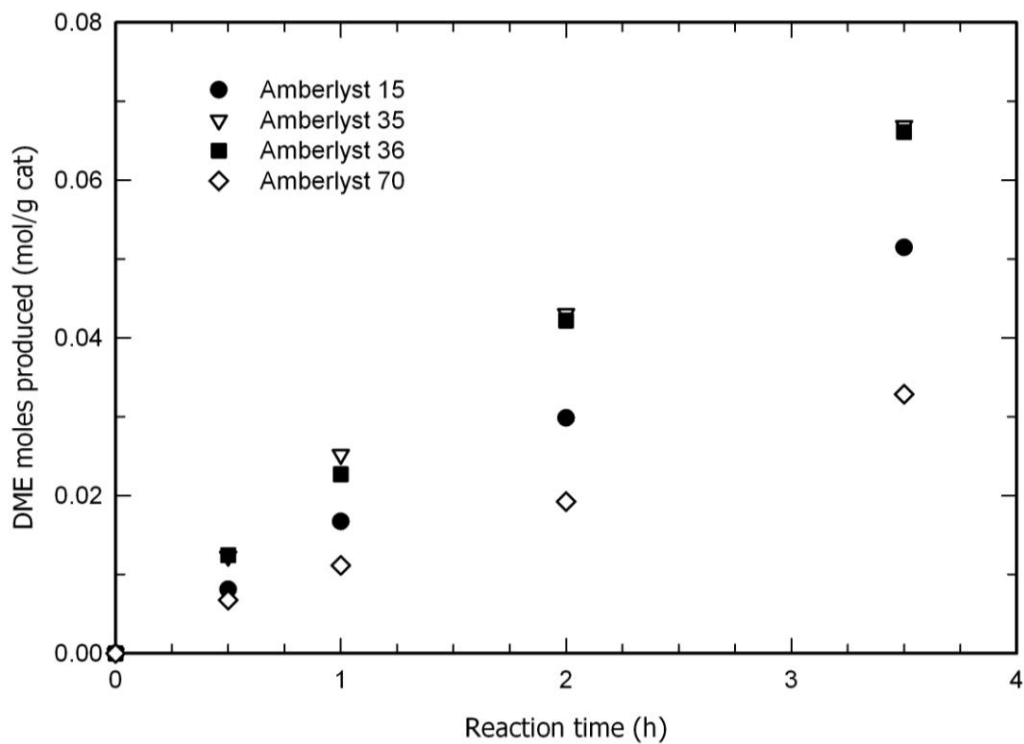


Figure 4.7 2.5M water in methanol solution as feed to reactor for methanol dehydration reaction over Amberlysts at 130 °C and 900kPa

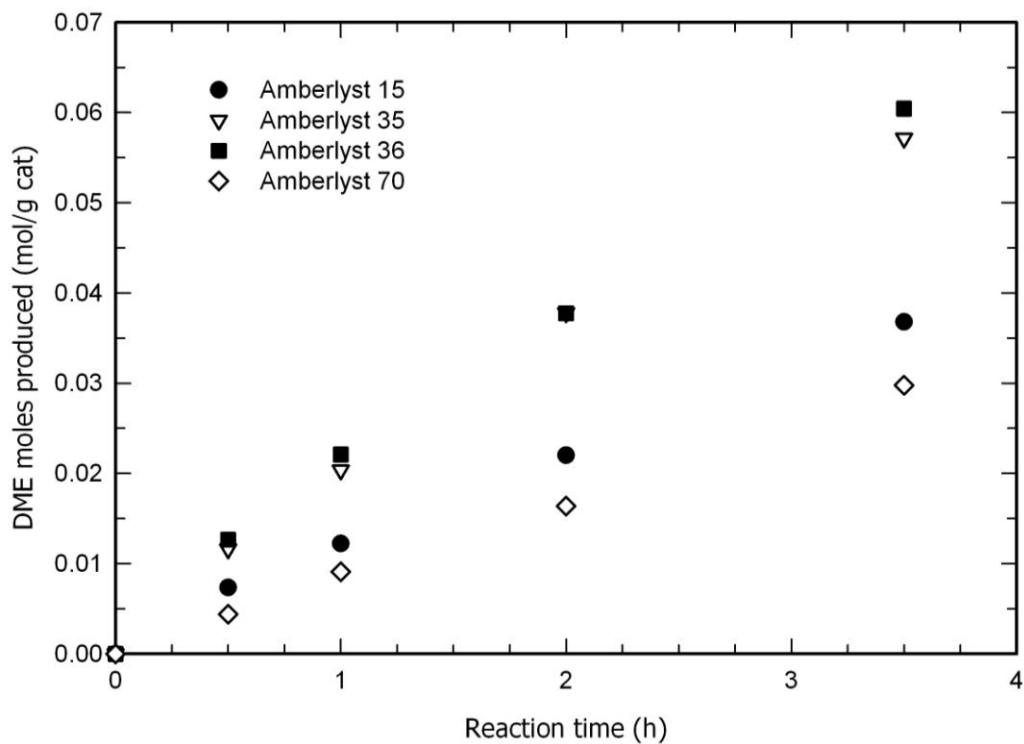


Figure 4.8 3.5M water in methanol solution as feed to reactor for methanol dehydration reaction over Amberlysts at 130 °C and 900kPa

Figure 4.9 shows the initial rates of reaction for Amberlyst 15, 35, 36 and 70 for pure methanol, 2.5 M and 3.5 M water concentrations in methanol. The initial rate of reaction for each catalyst was obtained using nonlinear regression between the DME moles produced and the reaction time data shown in Figure 4.6 to Figure 4.8. The initial rate of the reaction is equal to the value of the derivative at time 0. This figure also shows that Amberlyst 35 and 36 have higher initial rate and show more activity than that Amberlyst 15 and 70 for pure methanol and for both water concentrations.

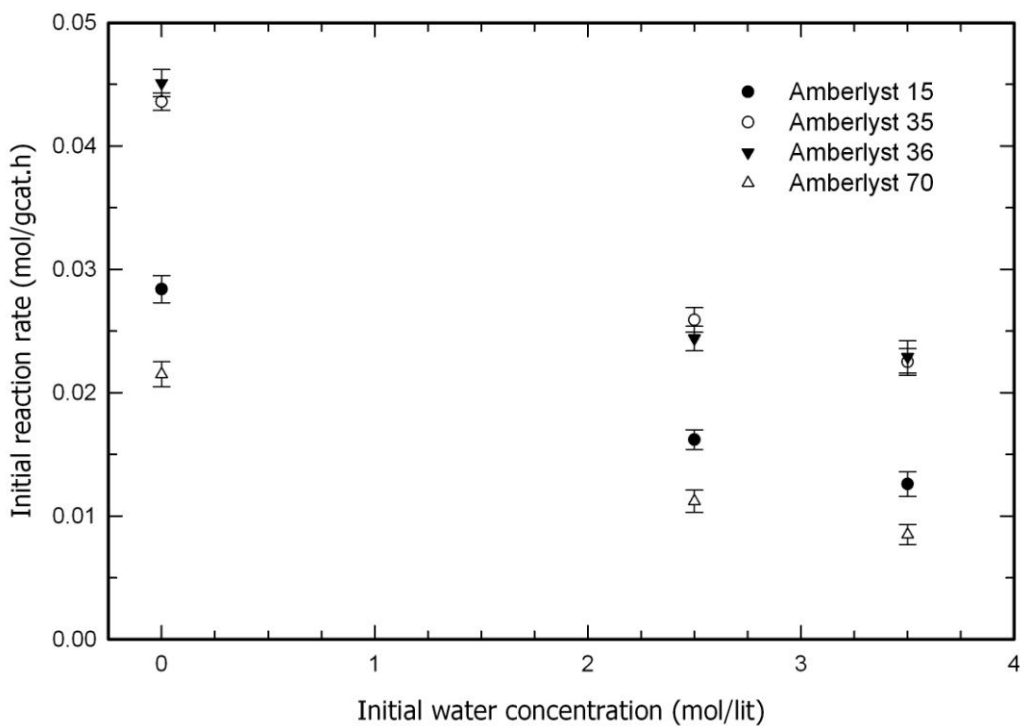


Figure 4.9 Initial reaction rate for pure methanol, 2.5M and 3.5M water solutions over Amberlyst 15, 35, 36 and 70 at 130 °C and 900kPa

Figure 4.10 shows the correlation between the initial rate of the reaction at 110 °C and the acidity capacity of Amberlyst catalysts. It can be seen that there is a direct relationship between the initial reaction rate and the acidity of the catalyst. As the acidity of the catalyst increases, the rate of reaction increases.

These preliminary investigations show that Amberlyst 35 and 36 have shown higher DME production and consequently higher initial rate of reaction at lower reaction temperatures and higher initial water concentrations than Amberlyst 15 and 70. Although, both Amberlyst 35 and 36 shown very similar activity Amberlyst 35 has more crosslinks and less swelling than that Amberlyst 36. Amberlyst 35 has better catalytic properties and physical stability. Thus, we chose Amberlyst 35 for further kinetics studies.

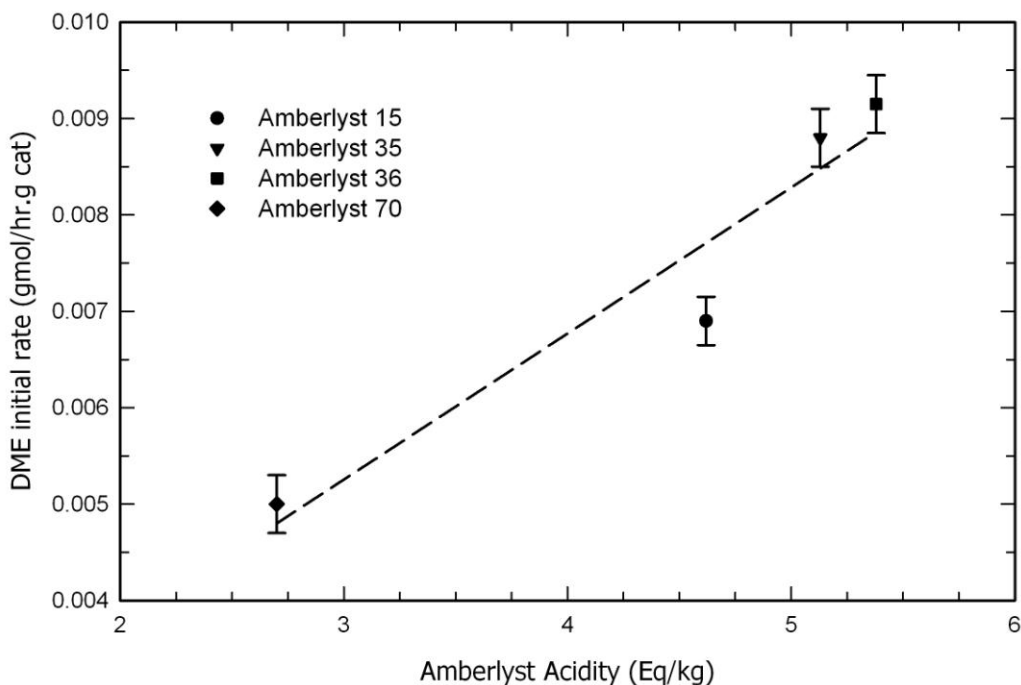


Figure 4.10 The initial reaction rate of DME production as a function of catalyst acidity for Amberlyst 15, 35, 36 and 70 at 110 °C using pure methanol as feed

4.1. Kinetic Studies for Amberlyst 35

To determine a model to describe the kinetics of dehydration of methanol to DME, a series tests was also performed to examine, the effects of the initial mass reactant to catalyst mass ratio, external and internal diffusion, and finally reaction pressure on the initial reaction rate. Furthermore, the reproducibility the reaction was also examined by repeating one of run four more times. Total time for

experiment is considered to be 3.5 hr with liquid samples taken at 30, 60, 120, and 210 min.

4.1.1. Reproducibility

For each test of four runs, 4 g Amberlyst and 120 g methanol were charged into the reactor, which was pressurized to 900 kPa and heated up to 130 °C. The liquids samples were taken at 0, 30, 60, 120 and 210 minutes. Each liquid sample was taken twice. Table 4.1 and Figure 4.11 show that the amount of DME produced for each run are very similar. In fact the maximum deviation is less than 4% for four runs that conducted. This indicates that the kinetics results are quite consistent.

Table 4.1 Comparison of DME produced as a function of time for four runs

Time (min)	DME moles (mol/gcat)				Average	Max diff	Deviation %
	1	2	3	4			
30	0.0250	0.0263	0.0267	0.0273	0.0263	0.0010	3.7
60	0.0439	0.0450	0.0469	0.0467	0.0456	0.0013	2.8
120	0.0725	0.0745	0.0763	0.0768	0.0750	0.0017	2.3
240	0.1059	0.1089	0.1048	0.1083	0.1070	0.0019	1.8

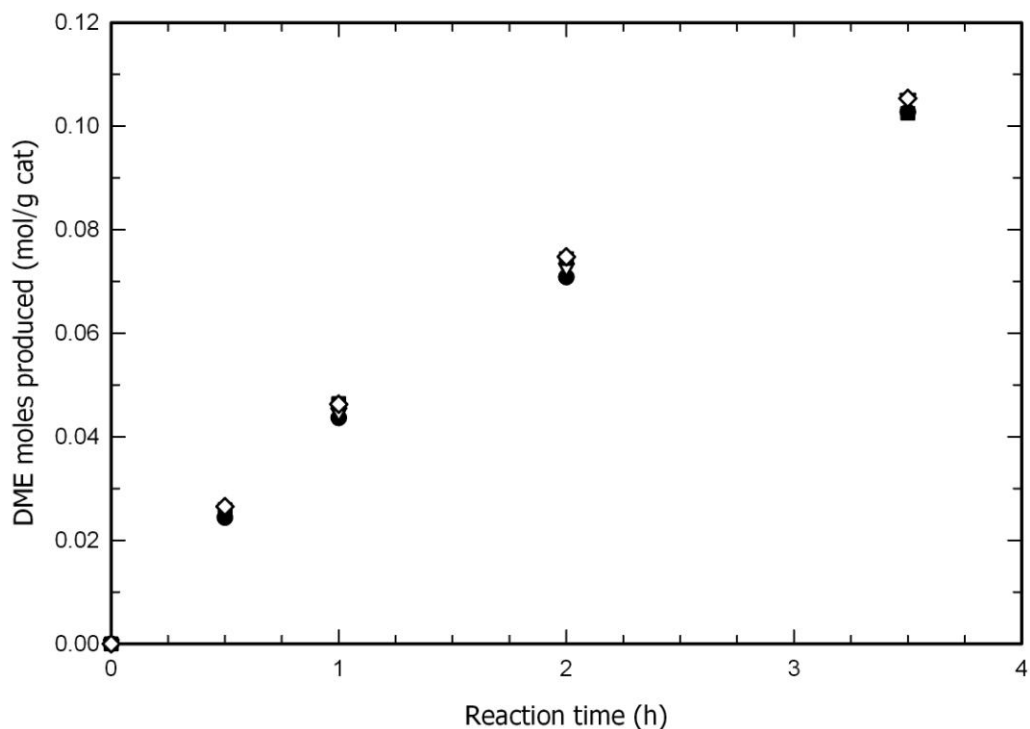


Figure 4.11 Moles of DME produced at 130 °C and 900 kPa using pure methanol as feed for four runs

4.1.2. The effect of initial reactant mass to catalyst mass ratio

It is expected that with increasing the amount of catalyst, the production rate of DME should increase. Three tests were conducted for catalyst (Amberlyst 35) amounts of 4 , 6 and 8 g while keeping the initial methanol amount constant. For each test, 120 g methanol was charged into the reactor and pressurized to 900 kPa and heated to 130 °C. The produced DME as a function of reaction time for methanol masses to catalyst mass ratios of 30, 20 and 15 are shown in Figure 4.10. It can be seen that as the ratios of methanol mass to catalyst mass increased from 15 to 30 the amount of produced DME per gram of catalyst increased. For higher ratios (i.e. less catalyst amount), less amount of water is produced, which result in less inhibiting effect on reaction rate. The initial rate of reaction for each ratio of reactant mass to catalyst mass was also obtained using nonlinear regression between the DME produced and the reaction time data shown in Figure

4.12. Table 4.2 shows a summary of the initial reaction rates and methanol conversions for three different ratios of reactant mass to catalyst mass. Table 4.2 shows that for all three ratios, the initial reaction rates per gram of catalysts are similar. Table 4.2 also shows that as the ratio of methanol mass to catalyst mass increases from 15 to 30 the methanol conversion increases as expected. For higher ratios (i.e. less catalyst amount), less amount of water is produced, which result in less inhibiting effect on reaction rate and hence higher initial reaction rate.

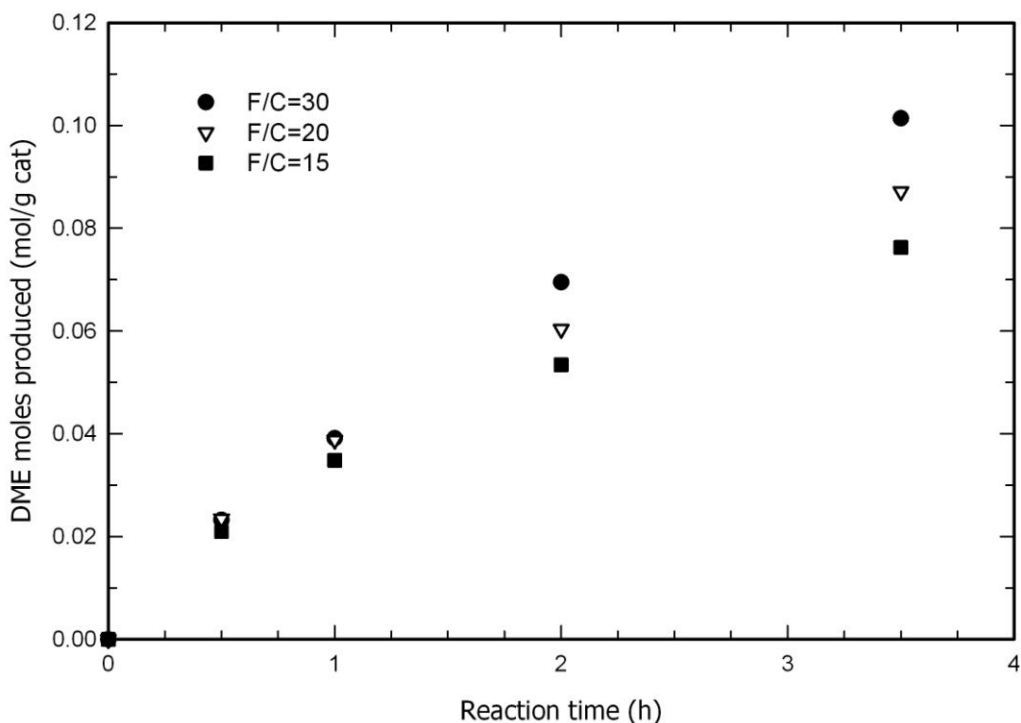


Figure 4.12 DME synthesized for different initial reactant mass/catalyst mass ratios of 120/4, 120/6, and 180/8 at 130 °C and 900 kPa using pure methanol as feed

Another experiment with the same amount of feed mass to catalyst ratio (i.e. 30) but different amount of catalyst and feed (i.e. 6 g and 180 g) was conducted. The result certifies that water concentration affects the reaction rate during the reaction.

Table 4.2 The initial reaction rate per gram of catalyst and final methanol % conversions for three different reactant mass to catalyst mass ratios.

Reactant mass/Catalyst mass	Initial rate of DME (mole/g cat.h)	Final methanol conversion (%)
30 (120/4)	0.0437 ±0.0009	22.2 ±1.5
20 (120/6)	0.0417 ±0.0007	28.9 ±1.4
15 (120/8)	0.0374 ±0.0006	33.8 ±1.4
30 (180/6)	0.0423 ±0.0011	20.7 ±1.5

4.1.3. The effect of external and internal diffusion

The external and internal diffusion could affect the kinetics of dehydration of methanol to DME. To study the effect of external diffusion on the reaction kinetics, two different tests with two different stirring speeds were conducted. It was found that for the stirring speeds of 750 rpm and 650 rpm the initial reaction rates were 0.047 and 0.046 mol/g cat.h, respectively as expected. It is well known that if the stirring speed is set sufficiently high the external diffusion is not a limiting factor.

The effect of internal diffusion limitation on overall kinetics of dehydration of methanol to DME was investigated by varying sizes of Amberlyst 35 catalyst pellets. In the present study, the particle size of Amberlyst 35 was varied from 0.2 mm to 0.6 mm. For two tests, the reactor was charged with 4 g Amberlyst 35 and 120 g methanol and pressurized to 900 kPa and heated to 130 °C. The stirrer speed was set to 750 rpm. Figure 4.13 shows that catalyst particle size has little effect on the rate of produced DME because Amberlyst 35 has significantly large average pore diameter as shown in Table 3.2. Therefore, we can conclude that internal diffusion has no effect or little effect on the overall kinetics of dehydration of methanol to DME.

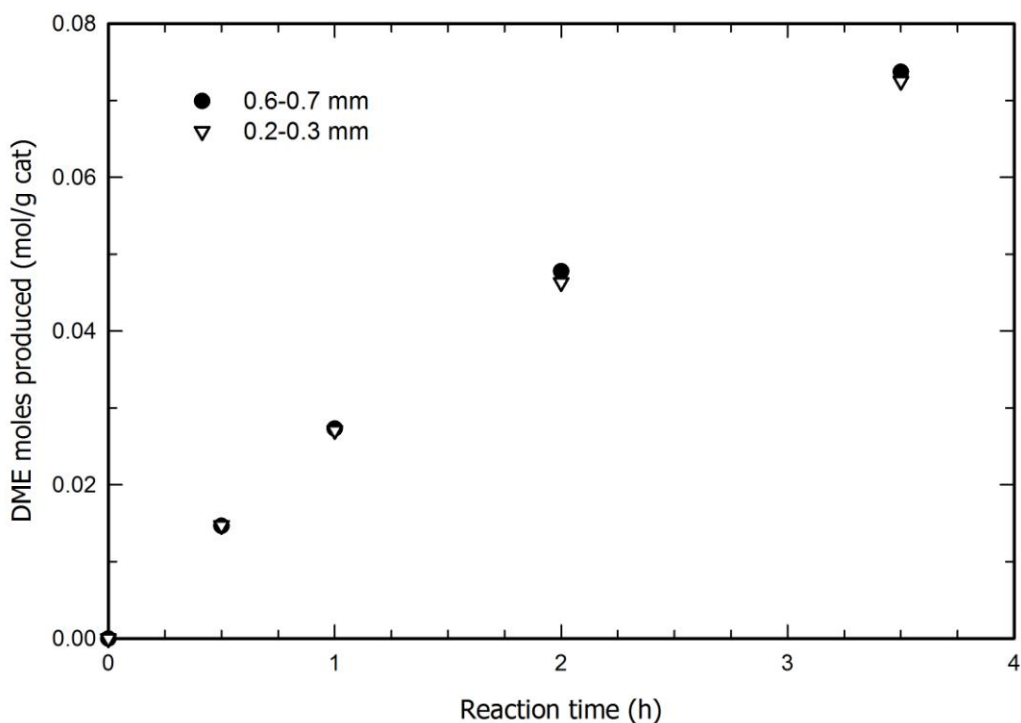


Figure 4.13 The DME produced moles over different Amberlyst catalyst particle sizes at 130 °C and 900 kPa using pure methanol as feed including the water from the catalyst

4.1.4. The effect of methanol concentration on reaction rate

To determine which model best describes the kinetics of the reaction; a series of experiments was performed to examine the effect of concentration of methanol and water on the initial rate of the reaction. For the first set of tests, methanol concentration was varied between 5 M and 24.6 M using tetrahydrofuran (THF) as an inert solvent. For temperatures of 110, 120, and 130 °C, the reactor was charged with 12, 8 and 4 g Amberlyst 35, respectively and 120 g of methanol/THF solutions. Figure 4.14 shows the effect of methanol concentration on the initial reaction rate for three temperatures. It is determined that the initial rate stayed relatively constant in the range of methanol concentrations investigated. This phenomenon can be explained by the Langmuir-Hinshelwood mechanism for the reaction where the surface reaction is the determining step. The mechanism proposed by Gates and Johanson (1971) states that two molecules

of methanol should occupy two adjacent acid sites in the catalyst; hence, the reaction can happen between those two molecules. According to Langmuir-Hinshelwood rate expression for this bi-molecular mechanism, the reaction rate is independent of methanol concentration in absence of water.

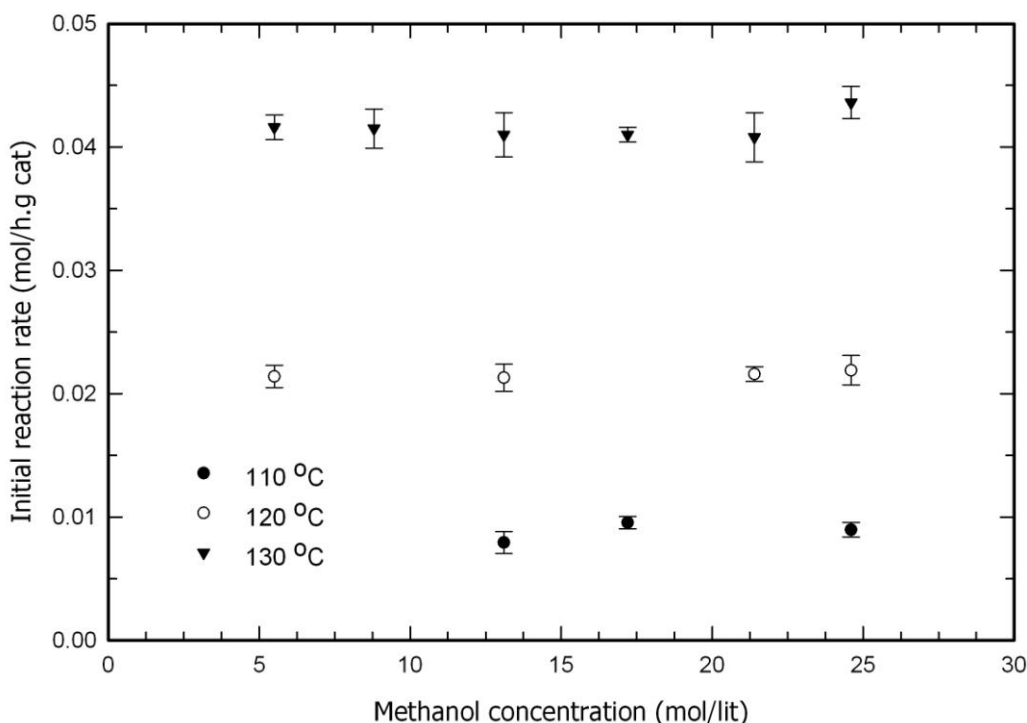


Figure 4.14 Effect of methanol concentration on initial reaction rate at different temperatures and 900 kPa for different concentrations of methanol/THF solutions

4.1.5. The effect of initial water concentration on reaction rate

In this set of tests, the initial water concentration in the reactor was varied from 0-3.5M to determine the effect of water concentration on the initial reaction rate. In these experiments, the reactor was charged with 4 g Amberlyst 35 catalyst and 120 g of 1.5, 2.5 and 3.5 M water/methanol solutions and then the reactor was pressurized to 900 kPa and heated to 130 °C. Figure 4.15 shows that water concentration has significant effect on the initial reaction rate. Water and methanol molecules compete for adsorption at catalytic active sites on the surface of Amberlyst 35. Hence, there is an inverse relationship of the initial reaction rate

and concentration of water in the reaction mixture (An et al., 2004; Kiviranta-Paakkonen et al., 1998).

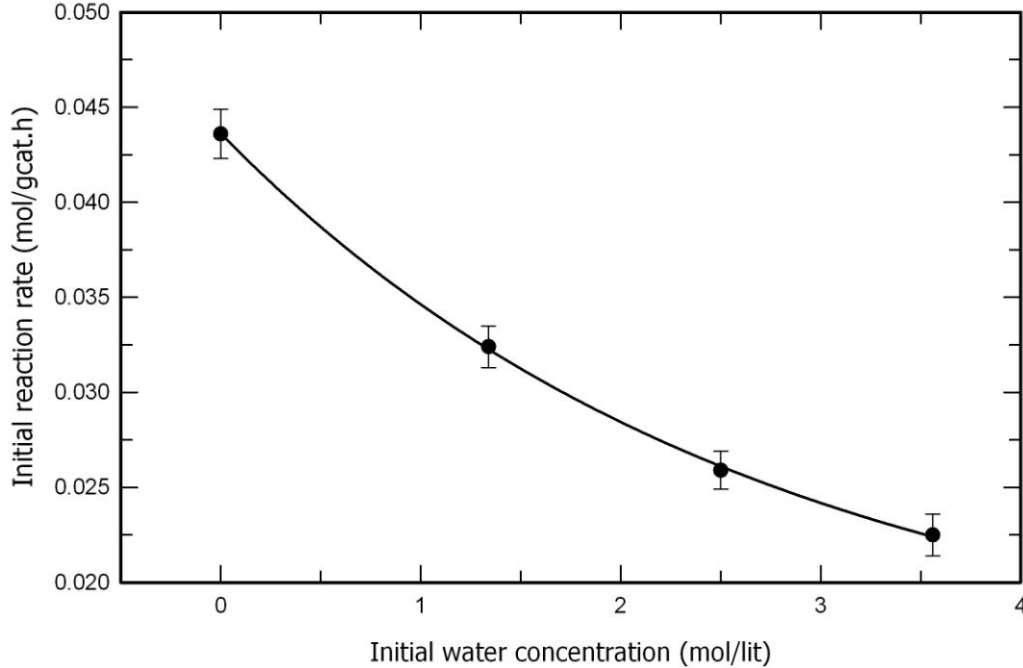


Figure 4.15 Effect of water concentration on initial reaction rate at 130 °C and 900 kPa using different concentrations of methanol/water solutions as feed

4.2. Kinetics Modeling

The kinetics of catalytic dehydration of methanol has been examined extensively in a gas-phase. This reaction mechanism has been found to follow Langmuir-Hinshelwood or Eley-Rideal type expressions. In present study, we will examine Langmuir-Hinshelwood and Eley-Rideal type of kinetics, which were proposed by Kiviranta et al. (1998), An et al. (2006) and Di Stanislao et al. (2007) for liquid-phase reaction and based on the surface reaction as the rate determining step, and incorporates the effect of competitive adsorption of water and methanol molecules:

$$\text{Model 1 (LH)} \quad r_{\text{DME}} = \frac{k_s K_M^2 C_M^2}{(1 + K_M C_M + (K_W C_W)^n + K_{\text{DME}} C_{\text{DME}})^2} \quad (4.1)$$

$$\text{Model 2 (ER)} \quad r_{\text{DME}} = \frac{k_S K_M^2 C_M^2}{(1 + K_M C_M + (K_W C_W)^n + K_D C_D)} \quad (4.2)$$

where k_S is the surface reaction rate constant, and K_M , K_W , and K_D , and C_M , C_W , and C_D are the adsorption equilibrium constants and concentration of methanol, water and DME, respectively. The value of n is set to 0.5, 1 and 2 for the selected model to compare the fit with the experimental data.

Adsorption of more polar components such as water and methanol to acid sites is much stronger than less polar components (DME) due to the significant difference in dielectric constants of the components (An et al. 2008). Furthermore, because of the low boiling temperature and high vapor pressure of DME compared to water and methanol, most of DME produced will be in the gas phase. Gogate et al. (1990) also study the same reaction in the liquid-phase and they concluded that $K_{\text{DME}} C_{\text{DME}}$ term is very small compared to other terms in Equations (4.1) and (4.2). Therefore, Equations (4.1) and (4.2) simplifies further to:

$$\text{Model 1 (LH)} \quad r_{\text{DME}} = \frac{k_S K_M^2 C_M^2}{(1 + K_M C_M + (K_W C_W)^n)^2} \quad (4.3)$$

$$\text{Model 2 (ER)} \quad r_{\text{DME}} = \frac{k_S K_M^2 C_M^2}{(1 + K_M C_M + (K_W C_W)^n)} \quad (4.4)$$

For the first set of tests, methanol concentration was varied between 5M and 24.6M using tetrahydrofuran (THF) as an inert solvent. In absence of water, Equations (4.3) and (4.4) can be written as:

$$\text{Model 1 (LH)} \quad r_{\text{DME}} = \frac{k_S K_M^2 C_M^2}{(1 + K_M C_M)^2} \quad (4.5)$$

$$\text{Model 2 (ER)} \quad r_{\text{DME}} = \frac{k_S K_M^2 C_M^2}{(1 + K_M C_M)} \quad (4.6)$$

Furthermore, we can linearize Equations (4.5) and (4.6) with respect to methanol concentration:

$$\text{Model 1 (LH)} \quad \left[\frac{C_M^2}{(r_{\text{DME}})_0} \right]^{0.5} = \frac{1}{\sqrt{k_S}} + \frac{K_M}{\sqrt{k_S}} C_M \quad (4.7)$$

$$\text{Model 2 (ER)} \quad \left[\frac{C_M^2}{(r_{\text{DME}})_0} \right] = \frac{1}{k_S} + \frac{K_M}{k_S} C_M \quad (4.8)$$

In order to determine which model fits our experimental data shown in Figure 4.14, the left hand side of the Equations (4.7) and (4.8) was plotted versus various methanol concentrations, C_M as shown in Figure 4.16 and Figure 4.17. Comparison of these figures indicates that the experimental data fits better with Langmuir-Hinshelwood (model 1) for the temperature range studied. Hence, the Langmuir-Hinshelwood was selected as the best model for our study.

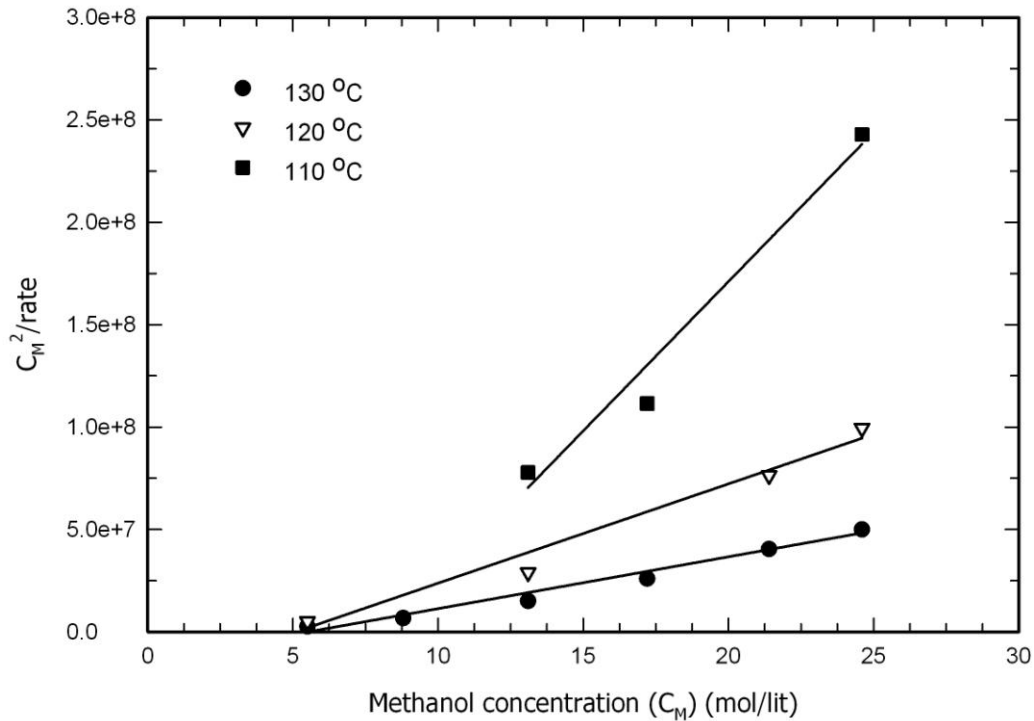


Figure 4.16 Left hand side of Equation (4.8) versus methanol concentration

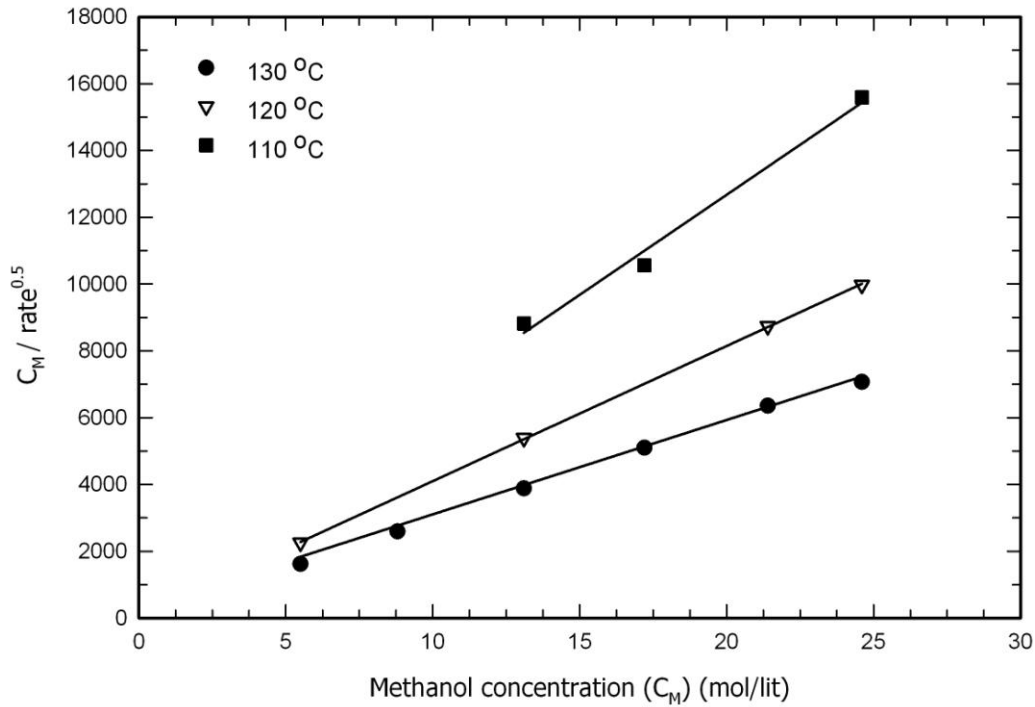


Figure 4.17 Left hand side of Equation (4.7) versus methanol concentration

Using a linear regression for data shown in Figure 4.16, the surface reaction rate constant, k_s and the adsorption equilibrium constants, K_M were determined. For higher methanol concentrations, the value obtained for $K_M C_M$ is significantly higher than 1 ($25 \gg 1$); thus, $1/\sqrt{k_s}$ term in Equation (4.7) is negligible compared to $K_M C_M / \sqrt{k_s}$ term. If we ignore the 1 in Equation (4.7) then the model can be simplified further

$$\text{Model 1 (LH)} \quad r_{\text{DME}} = \frac{k_s K_M^2 C_M^2}{(K_M C_M)^2} \Rightarrow r_{\text{DME}} = k_s \quad (4.9)$$

Since it was found that the methanol concentration had negligible effect on initial reaction rate, two more test were conducted at temperatures of 115 and 135 °C. Linear regression of the Arrhenius plot shown in Figure 4.18, the temperature independent parameters such as k_0 and E_a in Arrhenius equation (Equation (4.10)) were determined. The calculated values for k_0 and E_a are 6.12×10^7 (mol/s.kg cat)

and 98 (kJ/mol), respectively. The value of apparent activation energy is in accordance with the activation energy calculated by Kiviranta-Paakkonen et al. (1998) and Di Stanislao et al. (2007) which are 95 kJ/mol and 98 kJ/mol, respectively.

$$k_s = k_0 \exp\left(\frac{-E}{RT}\right) \quad (4.10)$$

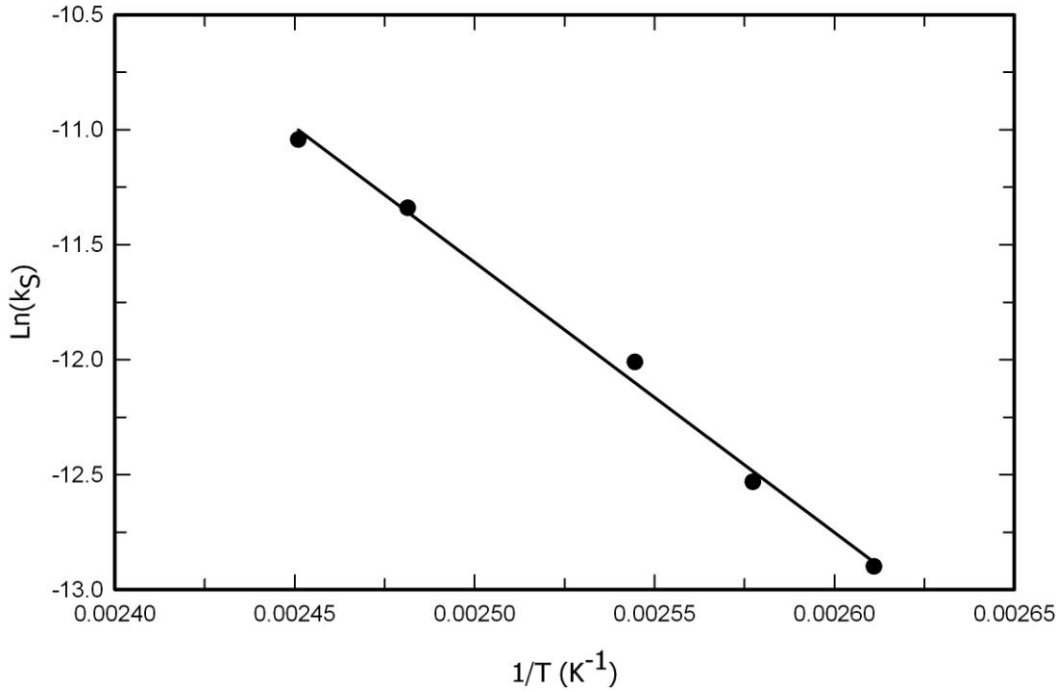


Figure 4.18 Arrhenius plot for methanol dehydration reaction at temperature range of 110 - 135 °C and 900 kPa using pure methanol as feed

In the presence of water, Equation (4.3) can be simplified for the second set of runs in last section,

$$r_{\text{DME}} = \frac{k_s K_M^2 C_M^2}{(K_M C_M + (K_W C_W)^n)^2} \quad (4.11)$$

Equation (4.11) can be further reorganized as

$$\frac{k_S}{r_{\text{DME}}} = \frac{(K_M C_M + (K_W C_W)^n)^2}{K_M^2 C_M^2} \quad (4.12)$$

Taking the square root of both sides of Equation (4.12), and dividing the nominator and denominator of the right hand side by $(K_M C_M)$ gives:

$$\frac{\sqrt{k_S}}{\sqrt{r_{\text{DME}}}} = 1 + \frac{(K_W C_W)^n}{K_M C_M} \quad (4.13)$$

To determine the best value of n in Equation (4.13) from the suggested values (i.e. 0.5, 1 and 2), set of experiments was conducted where water concentration was varied between 0-3.5 M at reaction temperature of 130 °C. The left hand side of Equation (4.13) was plotted versus $(C_W^{0.5}/C_M)$ and (C_W/C_M) as shown in Figure 4.19 and Figure 4.20, respectively. It can be seen from these two figures, when $n=1.0$, the linear regression line fits better to the experimental data. Thus Equation (4.13) can be written as:

$$\frac{\sqrt{k_S}}{\sqrt{r_{\text{DME}}}} = 1 + \frac{K_W}{K_M} \frac{C_W}{C_M} \quad (4.14)$$

The value for the surface reaction rate constant k_S calculated by linear regression of Equation (4.15) is 1.19 E-5 mol/kgcat.s at 130 °C, which is in good agreement with the value we obtained from the initial rates for the set of experiments conducted in absence of water (i.e. 1.21 E-5 mol/kgcat.s)

$$\frac{1}{\sqrt{r_{\text{DME}}}} = \frac{1}{\sqrt{k_S}} + \frac{1}{\sqrt{k_S}} \frac{K_W}{K_M} \frac{C_W}{C_M} \quad (4.15)$$

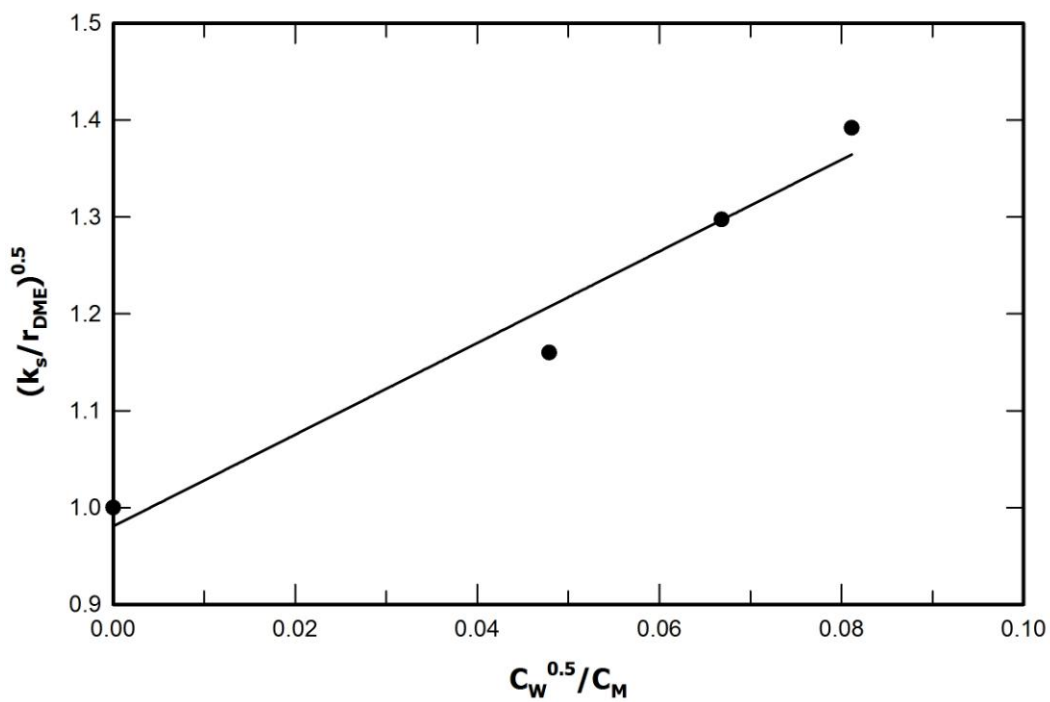


Figure 4.19 Left hand side of Equation (4.14) versus $(C_W^{0.5}/C_M)$

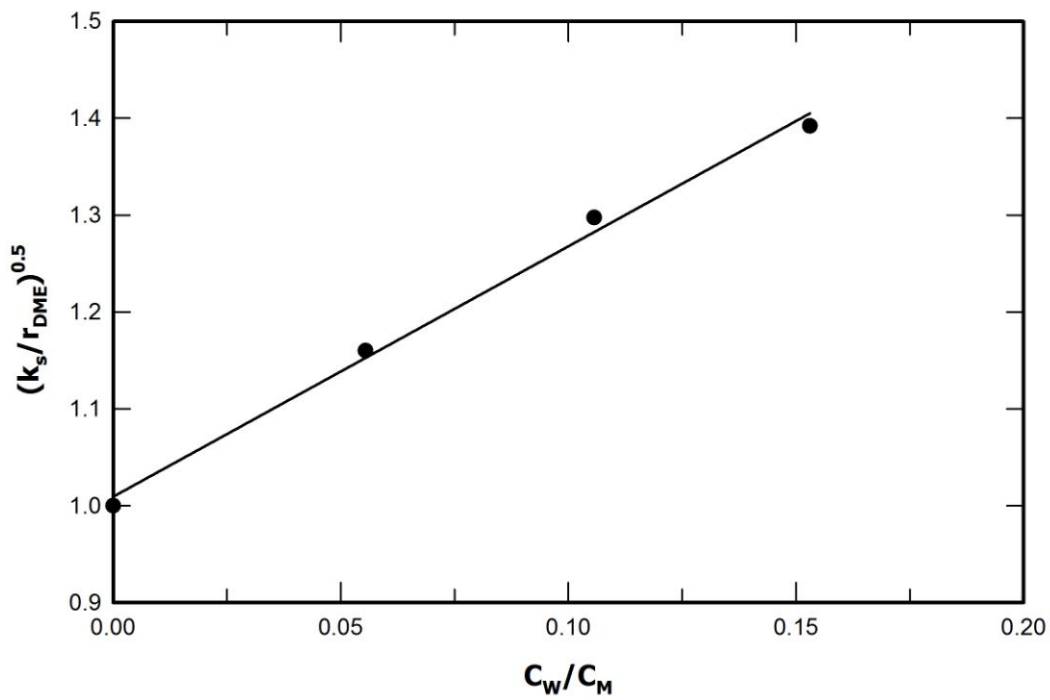


Figure 4.20 Left hand side of Equation (4.14) versus (C_W/C_M)

In Equation (4.14), K_W and K_M are temperature dependence adsorption equilibrium constants of water and methanol and can be defined using Van't Hoff relationship

$$K_W = K_{W0} \exp(-\Delta H_W / RT) \quad (4.16)$$

$$K_M = K_{M0} \exp(-\Delta H_M / RT) \quad (4.17)$$

The ratio of $\frac{K_W}{K_M}$ can be written as

$$\frac{K_W}{K_M} = K \exp(Q / RT) \quad (4.18)$$

where $K=(K_{W0}/K_{M0})$ and $Q=(\Delta H_M - \Delta H_W)$.

To determine K and Q in Equation (4.18), set of experiments was conducted using a constant water concentration (i.e. 3.5 M) with reactor temperature of 110, 115, 120, 130 and 135 °C. Using linear regression between $\ln(K_W / K_M)$ versus $1/T$ shown in Figure 4.21, K and Q values found to be 1.57×10^{-3} and 24.6 (kJ/mol), respectively. The temperature dependence of the ratio of adsorption equilibrium constants of water and methanol can be calculated with following equation.

$$\frac{K_W}{K_M} = \exp\left(-6.46 + \frac{2964}{T}\right) \quad (4.19)$$

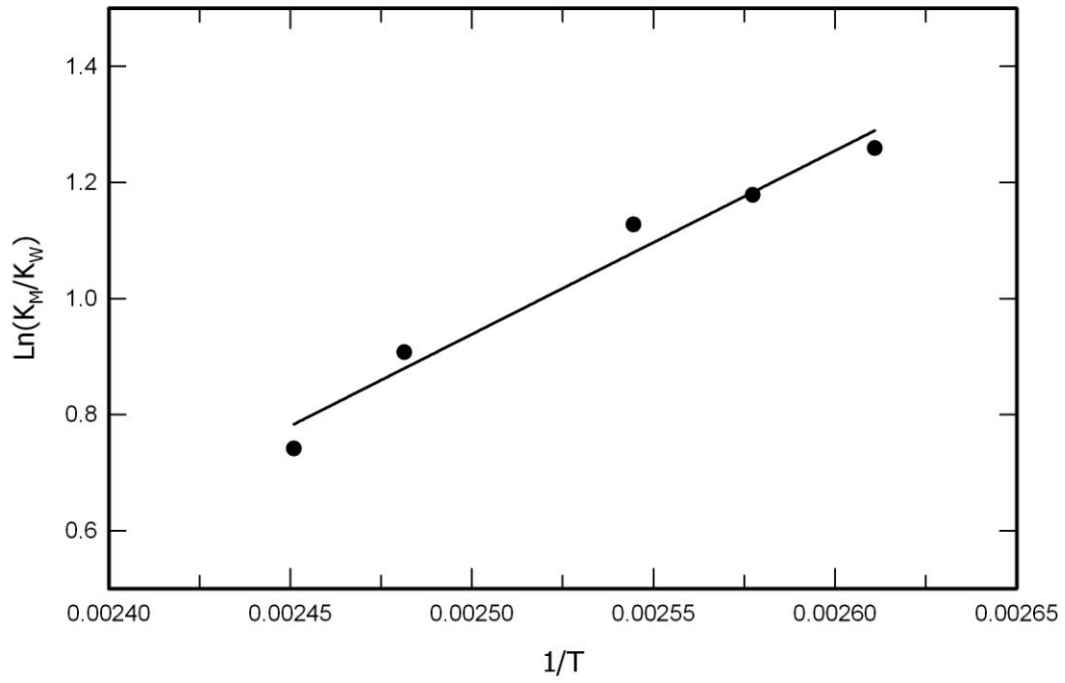


Figure 4.21 $\ln(K_M/K_W)$ versus $1/T$ in temperature range 110-135 °C and 900 kPa using 3.5 M water/methanol solution as feed

Chapter 5

Conclusion and Recommendations

The objective of this study was to investigate the catalytic dehydration of methanol to DME reaction with an outlook of implication in study of catalytic distillation for DME synthesis through methanol. The catalytic distillation of DME usually takes place at milder temperature and pressure. It was required to find a catalyst that requires relatively low temperature and pressure and shows high selectivity to DME production.

In present study, the activity of commercial solid-acid catalysts such as γ -Alumina, HY, HZSM-5, HM zeolites and ion exchange resins (Amberlyst 15, Amberlyst 35, Amberlyst 36, Amberlyst 70) for methanol dehydration to DME using a 500 ml Autoclave batch reactor was investigated. It was found that γ -Alumina and HY, HZSM-5, HM zeolites did not have a promising activity in the temperature range of 110-135 °C. However, ion exchange catalysts had significant activities. Further experiments over Amberlysts were conducted, and their behaviors for different temperatures and water concentrations were observed. Amberlyst 35 and 36 had similar activities in this set of experiments because of their close acidity amount; however, the Amberlyst 35 have better catalyst characteristics compared to Amberlyst 36 such as physical stability. Therefore, Amberlyst 35 was selected as the most practical catalyst for catalytic methanol dehydration, which requires relatively low operating conditions.

Kinetics of dehydration of methanol to DME over Amberlyst 35 was further tested in order to determine a reaction kinetic model. It was found that external diffusion was negligible with sufficiently high enough stirring speed and the internal diffusion cause no limitation due to large pore diameter of Amberlyst 35. Furthermore, methanol concentration did not have any effect on the reaction rate, which is in accordance with the mechanism proposed by Gates and Johanson (1971). In this mechanism, the two molecules of methanol, occupy two adjacent

acid sites, and the reaction happens between those molecules. Finally, It was also found that the presence of water had inhibiting effect on the reaction rate by competing with methanol molecules over acid sites.

In present study, we examined Langmuir-Hinshelwood and Eley-Rideal type of kinetics based on the surface reaction as the rate-determining step, and incorporated the effect of competitive adsorption of water and methanol molecules for Amberlyst 35 catalyst. It was found that the Langmuir-Hinshelwood model is the best fit for data. For the temperature range of 110-130°C and 900kPa, the final model and parameters found to be

$$r_{\text{DME}} = \frac{k_s K_M^2 C_M^2}{(K_M C_M + K_W C_W)^2} = \frac{k_s C_M^2}{\left(C_M + \frac{K_W}{K_M} C_W\right)^2} \quad (5.1)$$

where k_s is the surface reaction rate constant, and K_M/K_W , is the ratio of the adsorption equilibrium constants of water and methanol and found to be calculated by

$$k_s = 6.12E + 7 \exp\left(\frac{-98 \text{ kJ/mol}}{RT}\right) \quad (5.2)$$

$$\frac{K_W}{K_M} = \exp\left(-6.46 + \frac{2964}{T}\right) \quad (5.3)$$

In this study, the effect of some catalyst properties on its activity was investigated. In addition to these properties, the activity of Amberlyst for this reaction can be studied for various functional group acidity strengths. Spivey (1991) cited from Magnotta and Gates (1977) that the alcohol conversion increased by introducing Lewis acids to Amberlyst structure using AlCl_3 or BF_3 . Introducing Lewis acid to Brønsted acid sites produce super acids which are stronger functional group. This modified Amberlyst can be studied for this specific reaction to determine whether it increases the activity of the catalyst.

References

- An, W., Chuang, K. T., and Sanger, A. R. (2004). Dehydration of methanol to dimethyl ether by catalytic distillation. *The Canadian Journal of Chemical Engineering*, 82:948–955.
- Arcoumanis, C. Bae, C. Crookes, R. and Kinoshita, E. (2008). The potential of dimethyl ether (DME) as an *alternative* fuel for compression–ignition engines: a review. *Fuel*, 87.1014.
- Basu, A. Wainwright, J. (2001). DME as a power generation fuel: performance in gas turbines, *Petrotech-2001*, New Delhi.
- Bercic, G. and Levec, J. (1992). Intrinsic and global reaction rate of methanol dehydration over -alumina pellets. *Ind. Eng. Chem. Res.*, 31:1035.
- Cai, K.D., Yin, G.P., Zhang, J., Wang, Z.B., Du, C.Y. & Gao, Y.Z. (2008). Investigation of a novel MEA for direct dimethyl ether fuel cell, *Electrochemistry communications*, vol. 10, no. 2, pp. 238-241.
- Di Stanislao, M. Malandrino, A. Patrini, R. Viva, A. Brunazzi, E. (2007) Green Fuel Synthesis via Reactive Distillation, *Récents Progrès en Génie des Procédés, Numéro 94*, Ed. SPFG, Paris, France, p.p. 1-8
- Duarte de Farias, A., Esteves, A., Ziarelli, F., Caldarelli, S., Fraga, M., and Apple, L. (2004). *Appl. Surf. Sci.*, 227:132–138.
- Dupont, (1987). Toxicity summary for Dimethyl ether (DME); Dymel a propellant, Technical information.
- Dupont, (2000). Robust summary for Dimethyl ether, Prepared for U.S. EPA, Chemical right to know program.
- Endresen, Ø., Sjørgård, E., Sundet, J.K., Dalsøren, S.B., Isaksen, I.S.A., Berglen, T.F. & Gravir, G. (2003). Emission from international sea transportation and environmental impact, *J. Geophys. Res.*, vol. 108, no. D17, pp. 4560.
- Fei, J., Hou, Z., Zhu, B., Loy, H., and Zheng, X. (2006a). Synthesis of dimethyl ether (DME) on modified hy zeolite and modified hy zeolite-supported cu-mn-zn catalysts. *Applied Catalysis A: General*, 304:49–54.

Fei, J., Tang, X., Huo, Z., Luo, H., and Zheng, X. (2006b). Effect of copper content on Cu-Mn-Zn/Zeolite-Y catalysts for the synthesis of dimethyl ether from syngas. *Catalysis Communication*, 7:827–831.

Figoli, N., Hillar, S. & Parera, J. (1971), Poisoning and nature of alumina surface in the dehydration of methanol, *Journal of Catalysis*, vol. 20, no. 2, pp. 230-237.

Forster, P., V. Ramaswamy, P. Artaxo, T. Berntsen, R. Betts, D.W. Fahey, J. Haywood, J. Lean, D.C. Lowe, G. Myhre, J. Nganga, R. Prinn, G. Raga, M. Schulz and R. Van Dorland, (2007) Changes in Atmospheric Constituents and in Radiative Forcing. In: *Climate Change 2007: The Physical Science Basis. Contribution of Working Group I to the Fourth Assessment Report of the Intergovernmental Panel on Climate Change* [Solomon, S., D. Qin, M. Manning, Z. Chen, M. Marquis, K.B. Averyt, M. Tignor and H.L. Miller (eds.)]. Cambridge University Press, Cambridge, United Kingdom and New York, NY, USA.

Fu, Y., Hong, T., Chen, J., Auroux, A., and Chen, J. (2005). Surface acidity and the dehydration of methanol to dimethyl ether. *Thermochimica Acta*, 434:22–26.

Gates, B. and Johanson, L. (1969). The dehydration of methanol and ethanol catalyzed by polystyrene sulfonate resins, *Journal of Catalysis*, vol. 14, no. 1, pp. 69-76

Gates, B. and Johanson, L. (1971). Langmuir - Hinshelwood kinetics of the dehydration of methanol catalyzed by cation exchange resins. *AIChE Journal*, 17(4):981–983.

Ge, Q., Huang, Y., Qiu, F., and Li, S. (1998). Bifunctional catalysts for conversion of synthesis gas to dimethyl ether. *Applied Catalysis A*, 167(1):23–30.

Gogate, Makarand R., Lee, Byung Gwon, Lee, Sunggyu and Kulik, Conrad J. (1990). Kinetics of liquid phase catalytic dehydration of methanol to dimethyl ether, *Petroleum Science and Technology*, 8:6, 637-671

Good, D. A., J. S. Francisco, A. K. Jain, and D. J. Wuebbles (1998), Lifetimes and global warming potentials for dimethyl ether and for fluorinated ethers: CH₃OCF₃ (E143a), CHF₂OCHF₂ (E134), CHF₂OCF₃ (E125), *J. Geophys. Res.*, 103(D21), 28,181–28,186.

HaldorTopsøe, U.S. Patent 4,536,485, 1993 a

HaldorTopsøe, U.S. Patent 5,189,203, 1993 b

- Holman, J. & Gajda Jr, W. (1984). Experimental methods for engineers, 4th edition, Analysis of experimental data, p. 50, U.S., McGraw-Hill Book Company
- Jiang, S., Hwang, Y. K., Jhung, S. H., Chang, J.-S., Hwang, J.-S., Cai, T., and Park, S.-E. (2004b). Zeolite SUZ-4 selective dehydration catalyst for methanol conversion to dimethyl ether. *Chemistry Letters*, 33(8):1048–1049.
- Khandan, N., Kazemeini, M., and Aghaziarati, M. (2008). Determining an optimum catalyst for liquid phase dehydration of methanol to dimethyl ether. *Applied Catalysis A: General*, Accepted Manuscript
- Kim, E., Park, N., Kim, S., Joo, O., and Jung, K. (2004). DME synthesis from synthesis gas on the mixed catalysts of Cu/Zn/Al₂O₃ and ZSM-5. *Applied Catalysis A: General*, 264:37–41.
- Kim, S., Baek, S., Lee, Y., Jun, K., Kim, M., and Yoo, I. (2006). Effect of γ -alumina content on catalytic performance of modified zsm-5 for dehydration of crude methanol to dme. *Applied Catalysis A: General*, 309:139–143.
- Kiviranta-Paakkonen, P.K., Struckmann, L.K., Linnekoski, J.A., & Krause, A.O.I., (1998). Dehydration of the alcohol in the etherification of isoamylenes with methanol and ethanol, *Ind. Eng. Chem. Res.* 37, 18-24 (1998)
- Kline, S. J., and McClintock, F. A. (1953). Describing uncertainties in single-sample experiments, *Mech. Eng.*, P. 3
- Kozole, K.H., Wallace, J.S. (1988). The use of dimethyl ether as a starting aid for methanol-fuelled SI engines at low temperature. *SAE paper* 881677, October.
- Lee, E., Park, Y., Joo, O., and Jung, K. (2006). Methanol dehydration to produce dimethyl ether over γ -Al₂O₃. *React. Kinet. Catal. Lett.*, 89:115–121.
- Lee, S., Oh, S. & Choi, Y. (2009). Performance and emission characteristics of an SI engine operated with DME blended LPG fuel, *Fuel*, vol. 88, no. 6, pp. 1009-1015.
- Li, J.L., Zhang, X.G. & Inui, T. (1996). Improvement in the catalyst activity for direct synthesis of dimethyl ether from synthesis gas through enhancing the dispersion of CuO/ZnO/ γ -Al₂O₃ in hybrid catalysts, *Applied Catalysis A: General*, vol. 147, no. 1, pp. 23-33.

Li, K. & Jiang, D. (1999). Methanol synthesis from syngas in the homogeneous system, *Journal of Molecular Catalysis A: Chemical*, vol. 147, no. 1-2, pp. 125-130.

Lu, W., Teng, L., and Xiao, W. (2004). Simulation and experimental study of dimethyl ether synthesis from syngas in a fluidized bed reactor. *Chem. Eng. Sc.*, 59:5455–.

Magnotta, V. & Gates, B. (1977) Superacid polymers: Paraffin isomerization and cracking in the presence of AlCl₃-sulfonic acid resin complexes, *Journal of Catalysis*, vol. 46, no. 3, pp. 266-274

Marchionna, M., Patrini, R., Sanfilippo, D. & Migliavacca, G. (2008). Fundamental investigations on di-methyl ether (DME) as LPG substitute or make-up for domestic uses, *Fuel Processing Technology*, vol. 89, no. 12, pp. 1255-1261.

Mekasuwandumrong, O., silveston, P., Praserttham, P., Inoue, M., Pavarajam, V., and Tanakulrungsank, W. (2003). *Inorganic Chemistry Communication*, 6:930.

Meshkini, F., Taghizadeh, M. & Bahmani, M. (2010). Investigating the effect of metal oxide additives on the properties of Cu/ZnO/Al₂O₃ catalysts in methanol synthesis from syngas using factorial experimental design, *Fuel*, vol. 89, no. 1, pp. 170-175.

Minteer, Sh. (2006) *Alcoholic fuels*, U.S., CRC Press

Mollavali, M., Yaripour, F., Atashi, H., and Sahebdelfar, S. (2008). Intrinsic kinetics study of dimethyl ether synthesis on -Al₂O₃. *Ind. Eng. Chem. Res.*, 47:3265–3273.

Montgomery, D. C., Runger, G.C. (2007) *Applied statistics and probability for engineers*, 4th edition, p 270, John Wiley and Sons, Inc.

Moreno-Castilla, C., Carrasco-Marn, F., Parejo-Prez, C., and Ramn, M. V. L. (2001). Dehydration of methanol to dimethyl ether catalyzed by oxidized activated carbons with varying surface acidic character. *Carbon*, 39(6):869–875.

Ng, K., Chadwick, D., and Toseland, B. (1999). Kinetics and modelling of dimethyl ether synthesis from synthesis gas. *Chemical Engineering Science*, 54:3587–3592.

Olah, G.A. Goepfert, A. Surya Prakash, G.K. (2009) Beyond Oil and Gas: The Methanol Economy, 2nd edition, Methanol and Dimethyl Ether as Fuels and Energy Carriers, pp. 185-231, Germany, WILEY-VCH

Paas, M. (1997). Safety assessment of DME fuel, prepared for the transportation development center, Safety and Security Transport Canada, TP 12998E

Padmanabhan, V. & Eastburn, F. (1972) Mechanism of ether formation from alcohols over alumina catalyst, *Journal of Catalysis*, vol. 24, no. 1, pp. 88-91.

Ramos, F., de farias, A. D., Borges, L., Monteiro, J., Fraga, M., Sousa-Aguiar, E., and Appel, L. (2005). Role of dehydration catalyst acid properties on one-step dme synthesis over physical mixtures. *Catalysis Today*, 101:39–44.

Semelsberger, T., Ott, K., Borup, R., and Greene, H. (2005). Role of acidity on the hydrolysis of dimethyl ether (DME) to methanol. *Applied Catalysis B: Environmetal*, 61:281 – 287.

Semelsberger, T.A., Borup, R.L. & Greene, H.L. 2006, "Dimethyl ether (DME) as an alternative fuel", *Journal of Power Sources*, vol. 156, no. 2, pp. 497-511

Spivey, J. (1991). Review: Dehydration catalysts for the methanol/dimethyl ether reaction. *Chem. Eng. Comm.*, 110:123–142.

Sun, K., Lu, W., Qiu, F., Liu, S. & Xu, X. (2003). Direct synthesis of DME over bifunctional catalyst: surface properties and catalytic performance, *Applied Catalysis A: General*, vol. 252, no. 2, pp. 243-249.

Sun, Q., Fu, Y., Yang, H., Aline, A., and Shen, J. (2007). Dehydration of methanol to dimethyl ether over Nb₂O₅ and NbOPO₄ catalysts : Microcalorimetric and FT-IR studies. *Journal of molecular catalysis. A, Chemical*, 275:183–193.

Takegushi, T., Yanagisawa, K., Inui, T., and Inoue, M. (2000). Effect of the property of solid acid upon syngas to dimethyl ether conversion on the hybrid catalysts composed of Cu-Zn-Ga and solid acids. *Applied Catalysis A*, 192:201–209.

Thornton, R. & Gates, B. (1974). Catalysis by matrix-bound sulfonic acid groups: olefin and paraffin formation from butyl alcohols, *Journal of Catalysis*, vol. 34, no. 2, pp. 275-287.

Topp-Jorgensen, J. US Patent, 4,536,485, 1985, to Haldor Topsøe A/S, Denmark

Vishwanathan, V., Jun, K., Kim, J. W., and Roh, H. (2004a). Vapour phase dehydration of crude methanol to dimethyl ether over Na-modified H-ZSM-5 catalysts. *Applied Catalysis A: General*, 276:251–255.

Vishwanathan, V., Roh, H., Kim, J., and Jun, K. (2004b). Surface properties and catalytic activity of TiO₂-ZrO₂ mixed oxides in dehydration of methanol to dimethyl ether. *Catalysis Letter*, 96:23.

Xia, J., Mao, D., Zhang, B., Chen, Q., and Tang, Y. (2004). One-Step Synthesis of Dimethyl Ether from Syngas with Fe-Modified Zeolite ZSM-5 as Dehydration Catalyst. *Catalysis Letter*, 98:235–240.

Xia, J., Mao, D., Zhang, B., Chen, Q., Zhang, Y., and Tang, Y. (2006). Catalytic properties of fluorated alumina for production of dimethyl ether. *Catalysis Communication*, 7:362–366.

Xu, M., Goodman, D., and Bhattacharyya, A. (1997a). Catalytic dehydration of methanol to dimethyl ether (DME) over Pd/Cab-O-Sil catalysts. *Applied Catalysis A:General*, 149:303–309.

Xu, M., Lunsford, J., Goodman, D., and Bhattacharyya, A. (1997b). Synthesis of dimethyl ether (DME) from methanol over solid-acid catalysts. *Applied CatalysisA: General.*, 149:289–301.

Yaripour, F., Baghaei, F., Schmidt, I., and Perregaard, J. (2005a). Catalytic dehydration of methanol to DME over solid acid catalysts. *Catalysis Communication*, 6:147 – 152.

Yaripour, F., Baghaei, F., Schmidt, I., and Perregaard, J. (2005b). Synthesis of dimethyl ether from methanol over aluminium phosphate and silicatitania catalysts. *Catalysis Communication*, 6(2):542–549.

Zhang, Q., Li, X. & Fujimoto, K. (2006). Pd-promoted Cr/ZnO catalyst for synthesis of methanol from syngas, *Applied Catalysis A: General*, vol. 309, no. 1, pp. 28-32.

Appendix A

Experimental data

Category	Run	Methanol (g)	water (g)	THF (g)	Catalyst type	Catalyst amount (g)	temperature (C)	Initial rate (mol/gcat.h)
Solid acids @ 150 °C	201	120	0	0	A70	4±0.01	150±1	0.0643 ±0.0017
	202	120	0	0	HM	4±0.01	150±1	0.0365 ±0.0011
	203	120	0	0	ZSM-5	4±0.01	150±1	0.0087 ±0.0012
Amberlysts @ 110 °C	204	120	0	0	A15	6±0.01	110±1	0.0064 ±0.00025
	205	120	0	0	A35	6±0.01	110±1	0.0083 ±0.0003
	206	120	0	0	A36	6±0.01	110±1	0.009 ±0.0003
	207	120	0	0	A70	6±0.01	110±1	0.0049 ±0.0003
Amberlysts @ 130 °C	211	120	0	0	A15	4±0.01	130±1	0.0284 ±0.0011
	212	120	0	0	A35	4±0.01	130±1	0.0436 ±0.0009
	213	120	0	0	A36	4±0.01	130±1	0.0451 ±0.0012
	214	120	0	0	A70	4±0.01	130±1	0.0215 ±0.0010
Water effect on Amberlysts activities	221	113.3	6.7 (2.5M)	0	A15	6±0.01	130±1	0.0162 ±0.0008
	222	113.3	6.7 (2.5M)	0	A35	6±0.01	130±1	0.0259 ±0.0010
	223	113.3	6.7 (2.5M)	0	A36	6±0.01	130±1	0.0244 ±0.0010
	224	113.3	6.7 (2.5M)	0	A70	6±0.01	130±1	0.0112 ±0.0009
	225	110.5	9.5 (3.5M)	0	A15	8±0.01	130±1	0.0126 ±0.0010
	226	110.5	9.5 (3.5M)	0	A35	8±0.01	130±1	0.0225 ±0.0011
	227	110.5	9.5 (3.5M)	0	A36	8±0.01	130±1	0.0229 ±0.0013
	228	110.5	9.5 (3.5M)	0	A70	8±0.01	130±1	0.0085 ±0.0008
	229	115	5 (1.34 M)	0	A35	4±0.01	130±1	0.0324 ±0.0011

Category	Run	Methanol (g)	water (g)	THF (g)	Catalyst type	Catalyst amount (g)	temperature (C)	Initial rate (mol/gcat.h)
reproducibility	301	120	0	0	A35	4±0.01	130±2	0.0468 ±0.0014
	302	120	0	0	A35	4±0.01	130±2	0.0482 ±0.0013
	303	120	0	0	A35	4±0.01	130±2	0.0509 ±0.0011
	304	120	0	0	A35	4±0.01	130±2	0.0505 ±0.0013
Catalyst to feed ratio	311	120	0	0	A35	6±0.01	130±1	0.0417 ±0.0007
	312	120	0	0	A35	8±0.01	130±1	0.0374 ±0.0006
	313	180	0	0	A35	6±0.01	130±1	0.0423 ±0.0011
Int. and Ext. Diff.	321	120	0	0	A35	4±0.01	130±1	0.0448 ±0.0010
	322	120	0	0	A35-Wet	5±0.01	130±1	0.0289 ±0.0011
	323	120	0	0	A35-Wet	6±0.01	130±1	0.0282 ±0.0013
THF @ 130 °C	401	120	0	0	A35	4±0.01	130±1	0.0436 ±0.0013
	402	100	0	20	A35	4±0.01	130±1	0.0408 ±0.0020
	403	80	0	40	A35	4±0.01	130±1	0.041 ±0.0006
	404	60	0	60	A35	4±0.01	130±1	0.041 ±0.0018
	405	40	0	80	A35	4±0.01	130±1	0.0415 ±0.0016
	406	100	0	20	A35	4±0.01	130±1	0.0416 ±0.0010
THF @ 120 °C	411	120	0	0	A35	6±0.01	120±1	0.0219 ±0.0012
	412	100	0	20	A35	6±0.01	120±1	0.0216 ±0.0006
	413	60	0	60	A35	6±0.01	120±1	0.0213 ±0.0011
	414	20	0	100	A35	6±0.01	120±1	0.0214 ±0.0009
THF @ 110 °C	421	120	0	0	A35	10±0.01	110±1	0.0090 ±0.0006
	422	80	0	40	A35	10±0.01	110±1	0.0096 ±0.0005
	423	60	0	60	A35	10±0.01	110±1	0.0079 ±0.0009
For Arrhenius plot	431	120	0	0	A35	8±0.01	115±1	0.013 ±0.0006
	432	120	0	0	A35	4±0.01	135±1	0.0576 ±0.0019
Water solution at different temperatures	441	110.5	9.5 (3.5M)	0	A35	10±0.01	110±1	0.0038 ±0.0003
	442	110.5	9.5 (3.5M)	0	A35	8±0.01	115±1	0.0058 ±0.0004
	443	110.5	9.5 (3.5M)	0	A35	6±0.01	120±1	0.0101 ±0.0004
	444	110.5	9.5 (3.5M)	0	A35	4±0.01	135±1	0.033 ±0.0015

Appendix B

Sample calculation and error analysis

In each experiment, the methanol conversion and DME moles produced are calculated. A sample of calculations and error analysis for experiment #212 is shown in the following.

In Table B.1, the methanol area percentages from the GC are averaged and the real methanol percentage of the samples is calculated using the calibration equation.

$$\text{Methanol mass \%} = 0.001832(\text{Area\%})^3 - 0.4993(\text{Area\%})^2 + 46.3(\text{Area\%}) - 1369$$

Table B.1 Calculating methanol mass % in each sample

Reaction time (h)	Average of GC area %	Methanol mass % in sample
0	99.47	99.27
0.5	98.31	97.76
1	97.40	96.67
2	95.36	94.40
3.5	92.71	91.75

Water mass fraction is calculated by

$$w_{\text{H}_2\text{O}} = 1 - (\text{methanol mass \%} / 100)$$

Hysys is implemented to estimate the initial liquid mass (W_0) of the reaction. This estimation is the amount of methanol in liquid phase in equilibrium with the vapor at the operating temperature and pressure. As described in Chapter 3, the total mass in the liquid phase for each time step is calculated by Equation (3.5) and the mass of DME produced in each time interval is measured by Equation (3.6). For instance, for time 0 and 0.5 h, the mass of produced DME is estimated to be

$$W_{\text{DME}}(0) = \frac{0.0073 \times 117 \left(\frac{46.07}{18.02} \right)}{\left[1 + 0.0073 \left(\frac{46.07}{18.02} \right) \right]} = 2.15$$

$$W_{\text{DME}}(30) = \frac{0.0224 \times 117 \left(\frac{46.07}{18.02} \right)}{\left[1 + 0.0224 \left(\frac{46.07}{18.02} \right) \right]} = 6.34$$

For time = 0, the initial mass of DME is negligible and is set to zero by subtracting the initial mass of DME from all the calculated values i.e. the mass at time 0.5 h is 4.19 g. The moles of DME produced per gram of catalyst (N_{DME}) are obtained by dividing DME mass by M_{DME} (46.07 g/mol) and weight of catalyst used in the experiment.

$$N_{\text{DME}} = \frac{W_{\text{DME}}}{W_{\text{Cat}} \cdot M_{\text{DME}}} = \frac{4.19 \text{ g}}{4 \text{ g} \times 46.07 \frac{\text{g}}{\text{mol}}} = 0.0227 \frac{\text{mol}}{\text{gcat}}$$

DME moles per gram catalysts for other time steps are obtained with the same procedure. The initial reaction rate, using a second degree polynomial regression forced through origin, is determined 0.0436 mol/h. g cat. Moreover, methanol conversion for each time step is calculated by Equation (3.8). For instance, for time 0.5 h, the methanol converted in the reaction is

$$\text{Methanol conversion} = \frac{114.8(0.9927) - 110.7(0.9776)}{114.8(0.9927)} = 5.05 \%$$

Table B.2 DME moles and methanol conversion for different samples

Reaction time (h)	Total liquid mass (g)	n_{DME} (mol/gcat)	Methanol conversion (%)
0	114.8	0.0000	0.00
0.5	110.7	0.0227	5.05
1	107.8	0.0381	8.58
2	102.4	0.0678	15.24
3.5	96.6	0.0989	22.23

The error in this experiment is calculated by the Holman method as explained in Chapter 3. First, the error in the DME moles, caused by uncertainties in GC values and mass of the liquid phase, is calculated by Equation (3.11).

Table B.3 Uncertainty of DME mass for different samples

Reaction time (h)	W_{DME} (mol/gcat)	$\frac{\partial W_{\text{DME}}}{\partial W_0}$	$\frac{\partial W_{\text{DME}}}{\partial w_{\text{H}_2\text{O}}}$	Uncertainty of W_{DME}
0	2.16	0.0014	736.8	0.037
0.5	6.33	0.0117	684.2	0.105
1	9.18	0.0247	649.4	0.201
2	14.64	0.0627	585.3	0.172
3.5	20.37	0.1213	521.6	0.376

The deviation for the initial reaction rate which is obtained through a second degree polynomial regression is calculated by Equation (3.14). As there is no explicit function for the curve fitting of the data in an experiment, the derivatives for each time step is calculated according to Equation (3.15). The deviation of the initial reaction rate (Δr_0) caused by the variation of the mass of DME (ΔW_{DME}) in each time step, is divided by the difference made in mass of DME in order to find the derivative.

$$\frac{\partial r_0}{\partial W_{\text{DME}}(t)} = \frac{r_{(W_{\text{DME}}(t)+\Delta W_{\text{DME}})} - r_{(W_{\text{DME}}(t))}}{\Delta W_{\text{DME}}}$$

Substituting the derivatives in the Equation (3.10)

$$u_R = \left[(0.034)^2 + (0.105)^2 + (0.098)^2 + (0.088)^2 \right]^{0.5} = 0.17$$

The error for the initial reaction rate is

$$u_{r_0} = \frac{0.17}{4 \text{ g cat} \times 46.07 \frac{\text{g}}{\text{mol}}} = 0.0009$$

The initial rate for this experiment is 0.0436 ± 0.0009

Appendix C

Acidity measurements for Amberlysts

The acidity of the catalyst is measured according to the procedure supported by Rohm and Haas Co. One tenth of the values suggested by the procedure were used. For instance, 1.5 g of each Amberlyst is ion exchanged with 100 cm³ of sodium nitrate and 100 cm³ of HCl in regeneration. The procedure includes passing sodium nitrate through the catalyst bed where the cation exchange takes place. After exchanging the hydrogen ions in catalyst with sodium, the Catalyst is washed and regenerated by HCl to ion exchange the sodium ions by hydrogen. The regenerated catalyst is again ion exchanged by sodium nitrate, and exact 100 cm³ of solution is collected, and titrated by standard NaOH solution. The average of titration values is used for the calculation of acidity of Amberlyst.

Acidity of Amberlyst 35:

To measure the MHC (Moister Holding Capacity) 60.0 gr of Amberlyst 35 was weighed, and using the vacuum dryer, it has been dried overnight. After drying the weight of the catalyst was 29.1 gr. Therefore, the MHC percent is

$$\text{MHC}\% = \frac{60-29.1}{60} \times 100 = 51.5\% \quad (\text{C.1})$$

The result of the procedure is

W_{moist}	1.501 g
V_{moist}	2.00 cm ³
$V_{\text{As received, NaOH}}$	3.525 cm ³
N_{NaOH}	0.1122
$V_{\text{regen, NaOH}}$	3.325 cm ³
V_{blank}	0 cm ³

$$\text{Wt. Cap.} = \frac{10 \times (3.325 - 0) \times 0.1122}{1.501 \times (1 - 51.5/100)} = 5.13 (\text{Eq/kg}) \quad (\text{C.2})$$



ROHM AND HAAS COMPANY
Ion Exchange Resins

MASTER TEST METHODS

MTM 0265: CATION SALT SPLITTING CAPACITY AND PERCENT REGENERATION: H form resins

Objective

To determine the total exchange capacity of cation exchange resins on a weight (eq/kg) and volume (eq/L) basis. Also determine the percent regeneration.

Area of Application

This procedure is applicable to strong acid cation resins with sulfonic acid functional groups in the hydrogen form.

Principle

A sample of resin is pretreated as for the Moisture Holding Capacity. A known weight and volume of resin is eluted with NaNO_3 and the quantity of H determined by titration with NaOH. This provides the initial quantity of H present. The resin is then fully converted to the H form, the H is eluted with NaNO_3 , and the quantity of H is determined by titration with NaOH. This provides the strong acid, or salt splitting, capacity. This capacity is assumed equivalent to the total capacity for cation resins with sulphonic acid functional groups.

Equipment

Dewatering apparatus.

Source of vacuum, 40 ± 2 torr below atmospheric pressure.

Analytical balance, ± 0.001 g precision or better.

Ventilated oven, 105 ± 2 °C.

Desiccator.

Tared weighing dishes.

25 ml graduated cylinder, Kimble 20022-25 or equivalent.

Fritted glass filter tube.

1 L volumetric flask.
100 ml pipet.
Equipment for NaOH titration.

Reagents

1.0 N HCl.
0.5 N NaNO₃.
0.1000 N NaOH, standardized.
Deionized water.
Phenolphthalein indicator solution (5 g/L), used only for manual titrations.

Master Test Method

1. Prepare resin by the Master Test Method procedure for MHC.
2. Measure and record the MHC (to nearest 0.1%).
3. Weigh out a 15.0 ± 0.5 g sample of the prepared resin. Record the resin weight as W_{moist} (to nearest 0.01 g).
4. Quantitatively transfer the sample to a 25 ml graduated cylinder.
5. Cover the resin with deionized water to the 25 ml mark.
6. Shake the sample gently for 30 sec.
7. Allow the resin to settle, then tap the base of the graduated cylinder until no further settling is observed. Record the resin volume as V_{moist} (to nearest 0.25 ml).
8. Quantitatively transfer the sample to a fritted glass filter tube.
9. Pass 1 L of 0.5 N NaNO₃ through the sample at a rate of 25 ml/min. Collect exactly 1 L of effluent in a clean 1 L volumetric flask.
10. Stopper the flask and mix the contents thoroughly by inverting at least 5 times.
11. Pipet a 100 ml sample of the NaNO₃ effluent into a titration beaker.
12. Titrate the sample for H using 0.1000 N NaOH. Record the titration volume as $V_{\text{As received, NaOH}}$ (to nearest 0.01 ml) and the NaOH normality as N_{NaOH} (to nearest 0.0001 eq/L).
13. Rinse the same resin sample with 200 ml of deionized water. Discard the rinsate.
14. Pass 1 L of 1.0 N HCl through the sample at a rate of 25 ml/min.

15. Rinse with 1 L of deionized water at a flow rate of 25 ml/min. At the end of the rinse, verify that the effluent is near neutral using indicator paper.
16. Pass 1 L of 0.5 N NaNO₃ through the sample at a rate of 25 ml/min. Collect exactly 1 L of effluent in a clean 1 L volumetric flask.
17. Stopper the flask and mix the contents thoroughly by inverting at least 5 times.
18. Pipet a 100 ml sample of the NaNO₃ effluent into a titration beaker.
19. Titrate the sample for H using 0.1000 N NaOH. Record the titration volume as V_{Regen, NaOH} (to nearest 0.01 ml).
20. Pipet a 100 ml sample of the NaNO₃ influent blank into a titration beaker.
21. Titrate the blank for H using 0.1000 N NaOH. Record the titration volume as V_{Blank, NaOH} (to nearest 0.01 ml).
22. Report results to 1 decimal place, i.e., 95.0 %.
23. Calculate

$$\text{Wt. Cap. (eq/kg)} = \frac{10 \times (V_{\text{Regen,NaOH}} (\text{ml}) - V_{\text{Blank,NaOH}} (\text{ml})) \times N_{\text{NaOH}} (\text{eq/L})}{W_{\text{moist}} (\text{g}) \times (1 - \text{MHC}(\%) / 100)} \quad (\text{C.3})$$

$$\text{Vol. Cap. (eq/L)} = \frac{10 \times (V_{\text{Regen,NaOH}} (\text{ml}) - V_{\text{Blank,NaOH}} (\text{ml})) \times N_{\text{NaOH}} (\text{eq/L})}{V_{\text{moist}} (\text{ml})} \quad (\text{C.4})$$

$$\text{Percent}_{\text{H}} \% = \frac{100 \times (V_{\text{Asreceived,NaOH}} (\text{ml}) - V_{\text{Blank,NaOH}} (\text{ml}))}{V_{\text{Regenerated,NaOH}} (\text{ml}) - V_{\text{Blank,NaOH}} (\text{ml})} \quad (\text{C.5})$$

24. Report capacity results to 2 decimal places, i.e., 5.00 eq/kg or 2.00 eq/L. Report regeneration to 1 decimal place, i.e., 95.0%.

Appendix D

Mechanism study for Amberlyst 35

The reaction of methanol dehydration over Amberlyst 35 takes place on the sulfonic functional groups. These functional groups are Brønsted acid sites, although the pair of electrons on the oxygen molecule of the group can play the role of a Lewis base by donating electron. In the reaction of methanol over Amberlyst 35 acid sites, there are a variety of the ways that they can react to produce dimethyl ether.

Two mechanisms proposed for this reaction are single site reaction (Kiviranta-Paakkonen, 1998) and dual site reaction (Gates and Johanson, 1969). In single site reaction mechanism, one molecule of methanol is adsorbed to the acid site of the catalyst, and reacts with the other molecule of methanol from the bulk liquid. The three steps of reactants adsorption, surface reaction and product desorption are shown in Figure D.1.

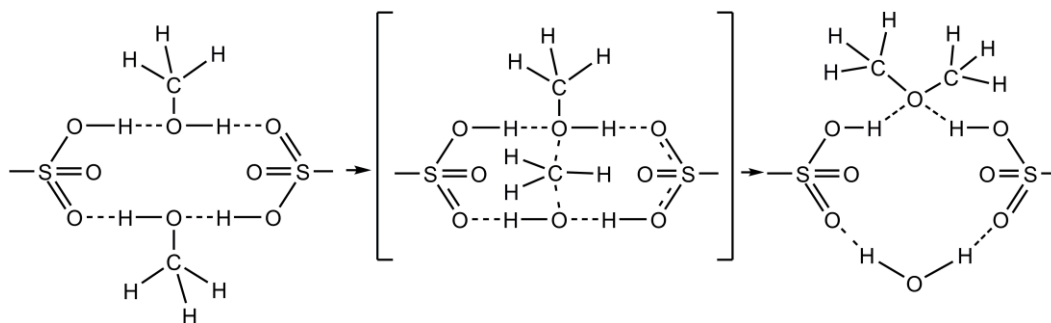


Figure D.1 Mechanism for dual site reaction model

On the other hand, dual site reaction mechanism states that two molecules of methanol are adsorbed to two adjacent acid sites where the reaction takes place. The three steps of reactants adsorption, surface reaction and product desorption are shown in Figure D.2.

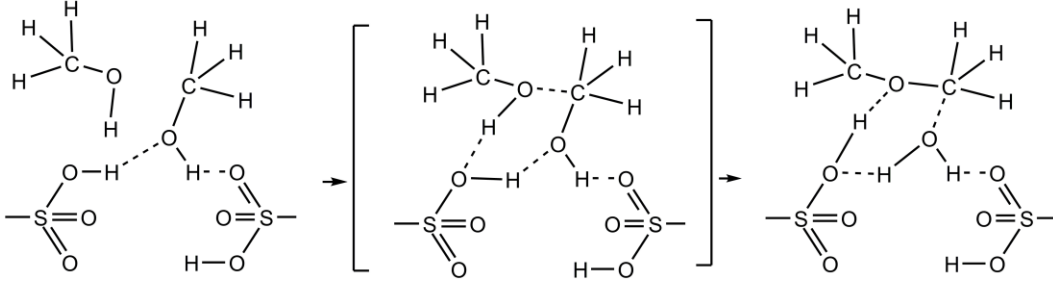


Figure D.2 Mechanism for single site reaction model

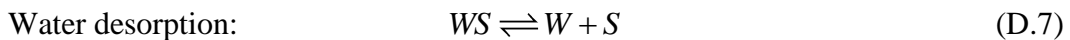
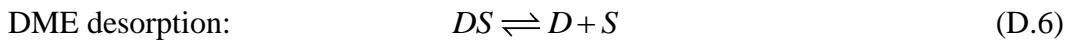
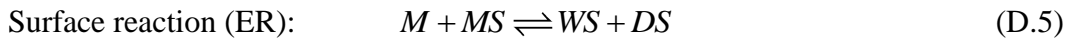
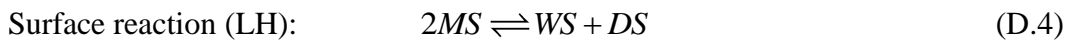
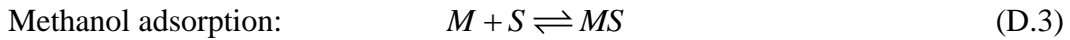
The model derived for the single site mechanism, known as Langmuir-Hinshelwood equation, is

$$r_{\text{DME}} = \frac{k_s K_M^2 C_M^2}{(1 + K_M C_M + K_W C_W + K_D C_D)^2} \quad (\text{D.1})$$

And the model for dual site reaction mechanism, known as Eley-Rideal equation, is

$$r_{\text{DME}} = \frac{k_s K_M C_M^2}{(1 + K_M C_M + K_W C_W + K_D C_D)} \quad (\text{D.2})$$

Following, it is shown how these models are derived from the mentioned mechanisms. There are three steps, i.e. methanol adsorption, surface reaction and water and DME desorption are



where M , W and D stand for methanol, water and DME molecule respectively and S is vacant acid site available for the reaction. MS , WS and DS are, respectively, methanol, water and DME molecules adsorbed to the occupied acid site. In LH

model two methanol molecules are adsorbed to the catalyst surface, but in ER model, one molecule reacts from the liquid phase.

The related rate function for each step is

$$\text{Methanol Adsorption: } r_{MA} = k_{MA} \left(C_M C_S - \frac{C_{MS}}{K_M} \right) \quad (\text{D.8})$$

$$\text{Surface reaction (LH): } r_S = k_S \left(C_{MS}^2 - \frac{C_{WS} \cdot C_{DS}}{K} \right) \quad (\text{D.9})$$

$$\text{Surface reaction (ER): } r_S = k_S \left(C_M C_{MS} - \frac{C_{WS} \cdot C_{DS}}{K} \right) \quad (\text{D.10})$$

$$\text{DME Desorption: } r_{DD} = k_{DD} \left(C_D C_S - \frac{C_{DS}}{K_D} \right) \quad (\text{D.11})$$

$$\text{Water Desorption: } r_{WD} = k_{WD} \left(C_W C_S - \frac{C_{WS}}{K_W} \right) \quad (\text{D.12})$$

where k_{MA} , k_S , k_{DD} and k_{WD} are rate constants and C_i is the concentration of component i in the solution.

Assuming surface reaction as the rate determining step, the other rate functions will be negligible (i.e. r_{MA} , r_{DD} , $r_{WD} = 0$).

$$\text{Methanol Adsorption: } r_{MA} = 0 \Rightarrow C_{MS} = K_M C_M C_S \quad (\text{D.13})$$

$$\text{DME Desorption: } r_{DD} = 0 \Rightarrow C_{DS} = K_D C_D C_S \quad (\text{D.14})$$

$$\text{Water Desorption: } r_{WD} = 0 \Rightarrow C_{WS} = K_W C_W C_S \quad (\text{D.15})$$

The total amount of acid sites is the sum of vacant acid sites and acid sites occupied by methanol, water and DME

$$C_T = C_S + C_{MS} + C_{WS} + C_{DS} \quad (\text{D.16})$$

Substituting Equation (D.13) to (D.15) in Equation (D.16) C_S can be written as

$$C_S = \frac{C_T}{(1 + K_M C_M + K_W C_W + K_D C_D)} \quad (\text{D.17})$$

Knowing that C_{MS} is $C_M C_S$, substituting Equation (D.17) into (D.9) gives

$$\text{Reaction rate (LH):} \quad r = \frac{C_T^2 k_S \left(K_M^2 C_M^2 - \frac{K_W K_D C_W C_D}{K} \right)}{(1 + K_M C_M + K_W C_W + K_D C_D)^2} \quad (\text{D.18})$$

$$\text{Reaction rate (ER):} \quad r = \frac{C_T k_S \left(K_M C_M^2 - \frac{K_W K_D C_W C_D}{K} \right)}{(1 + K_M C_M + K_W C_W + K_D C_D)} \quad (\text{D.19})$$

C_T as a constant can be combined by k_S to form k . In the case that the reverse reaction is negligible, reaction rates can be written as

$$\text{Reaction rate (LH):} \quad r = \frac{k K_M^2 C_M^2}{(1 + K_M C_M + K_W C_W + K_D C_D)^2} \quad (\text{D.20})$$

$$\text{Reaction rate (ER):} \quad r = \frac{k K_M C_M^2}{1 + K_M C_M + K_W C_W + K_D C_D} \quad (\text{D.21})$$